Mon. Not. R. Astron. Soc. **388,** 737–752 (2008) doi:10.1111/j.1365-2966.2008.13426.x

Two-fluid models of superfluid neutron star cores

N. Chamel★

Institut d'Astronomie et d'Astrophysique, Université Libre de Bruxelles, CP226, Boulevard du Triomphe, B-1050 Brussels, Belgium

Accepted 2008 May 7. Received 2008 April 10; in original form 2008 February 7

ABSTRACT

Both relativistic and non-relativistic two-fluid models of neutron star cores are constructed, using the constrained variational formalism developed by Brandon Carter and co-workers. We consider a mixture of superfluid neutrons and superconducting protons at zero temperature, taking into account mutual entrainment effects. Leptons, which affect the interior composition of the neutron star and contribute to the pressure, are also included. We provide the analytic expression of the Lagrangian density of the system, the so-called master function, from which the dynamical equations can be obtained. All the microscopic parameters of the models are calculated consistently using the non-relativistic nuclear energy density functional theory. For comparison, we have also considered relativistic mean field models. The correspondence between relativistic and non-relativistic hydrodynamical models is discussed in the framework of the recently developed 4D covariant formalism of Newtonian multifluid hydrodynamics. We have shown that entrainment effects can be interpreted in terms of dynamical effective masses that are larger in the relativistic case than in the Newtonian case. With the nuclear models considered in this work, we have found that the neutron relativistic effective mass is even greater than the bare neutron mass in the liquid core of neutron stars.

Key words: dense matter – equation of state – hydrodynamics – relativity – stars: neutron.

1 INTRODUCTION

The recent discovery of quasi-periodic oscillations (QPOs) in the X-ray flux of giant flares from soft-gamma repeaters (SGR) may well be the first direct observational evidence of neutron star oscillations. QPOs have been detected during the 2004 December 27 giant flare from SGR 1806−20 (Israel et al. 2005; Strohmayer & Watts 2006; Watts & Strohmayer 2006), during the 1998 August 27 giant flare from SGR 1900+14 (Strohmayer & Watts 2005) and during the 1979 March 5 event in SGR 0526−66 (Barat et al. 1983). Those QPOs are usually interpreted as global seismic vibrations triggered by magnetic crust quakes (for a recent review of these so-called magnetars, see e.g. Woods & Thompson 2006 and references therein). If this interpretation is confirmed, the analysis of those QPOs can potentially reveal the interior composition of neutron stars, thus putting constraints on the theory of dense matter (Samuelsson & Andersson 2007). Apart from QPOs in SGR, the rapid development of the gravitational wave astronomy opens very exciting perspectives of directly observing neutron star oscillations in a near future (Andersson & Kokkotas 2005). In particular, accreting neutron stars in Low-Mass X-ray Binaries are expected to be detectable by the Advanced Laser Interferometer Gravitational Wave Observatory (LIGO) detector[1] which is planned to be operational in a few years (see e.g. the recent analysis of Watts et al. 2008). However, the interpretation of these observations requires not only a detailed theoretical understanding of the dynamics of neutron stars, but also a consistent description of the different layers.

A neutron star is mainly composed of three distinct regions: an outer crust, an inner crust characterized by the presence of a neutron ocean and a liquid core which might be solid in the deepest regions (Haensel, Potekhin & Yakovlev 2006). Microscopic calculations of dense nuclear matter suggest that the matter inside neutron stars is superfluid (Dean & Hjorth-Jensen 2003). This theoretical prediction is strongly supported by the observations of pulsar glitches (Baym, Pethick & Pines 1969; Anderson & Itoh 1975). Other indications in favour of superfluidity, while less convincing, are provided by observations of neutron star thermal X-ray emission (Yakovlev & Pethick 2004). One of the remarkable consequences of superfluidity is the possibility of having several dynamically distinct components. The electrically charged particles inside neutron stars are locked together by the interior magnetic field and co-rotate on very long time-scales of the order of the age of the star (Easson 1979). The charged particles are rotating at the observed angular velocity of the star due to the coupling with the radiating magnetosphere and thus follow the long-term spinning-down of the star caused by the electromagnetic radiation. In contrast, the neutrons being electrically uncharged and superfluid can rotate at a different rate. This naturally leads to considering the interior of a neutron star as a two-fluid mixture. As a result of the strong interactions between neutrons

★E-mail: nchamel@ulb.ac.be

[1] http://www.ligo.caltech.edu/advLIGO/

and protons, the two fluids are not completely independent but are coupled via mutual entrainment effects. These non-dissipative effects are known to significantly affect the frequencies of superfluid oscillation modes for which the superfluid neutrons and the charged particles are counter moving (Andersson & Comer 2001). Two-fluid models of superfluid neutron star cores including entrainment effects have been proposed by Comer & Joynt (2003). Carter, Chamel & Haensel (2005, 2006b) (see also Chamel & Carter 2006) have shown how to describe in a unified way both the liquid core and the inner crust within this two-fluid picture. The description of the outer crust requires a different treatment (Carter, Chachoua & Chamel 2006a). Eventually, the different layers have to be matched with appropriate boundary conditions at the interfaces (Andersson, Comer & Langlois 2002; Lin, Andersson & Comer 2007).

In this work, we have constructed relativistic hydrodynamical models of cold superfluid neutron star cores, calculating *all* the necessary microscopic coefficients with the *same* underlying microscopic model. The present work differs from that of Comer & Joynt (2003) by improving the microphysics description of dense nuclear matter and by making the link between non-relativistic and relativistic models. In the first section, we briefly review the convective variational formalism of multifluid systems. This approach is employed to construct a two-fluid model of neutron star core in the Newtonian framework in Section 3. It is then shown in Section 4 how to generalize this model to relativistic fluids. In Section 5, we discuss the effects of entrainment in terms of dynamical effective masses. The consequences of superfluidity at the hydrodynamical scale are discussed in Section 6. Section 7 is devoted to the conditions of 'chemical' equilibrium and to the composition of neutron star cores. In Section 8, the microscopic parameters of the two-fluid model are evaluated, using Skyrme effective nucleon–nucleon interactions. As an example, numerical results are shown in Section 9 for three particular Skyrme forces: the popular SLy4 force and the parameter sets LNS and NRAPR which were entirely constructed from realistic quantum many-body calculations. In Section 10, results are compared to those obtained by the relativistic mean field theory applied by Comer & Joynt (2003). We have constructed new relativistic mean field models that yield a much better agreement with nuclear data than those considered by Comer & Joynt (2003).

2 VARIATIONAL FORMALISM OF MULTIFLUID HYDRODYNAMICS

In the following, we will use Greek letters for the space–time indices μ, ν, ... and Latin letters i, j, ... for space indices. We introduce capital Latin letters X, Y for distinguishing the various constituents and among them we will adopt the symbols ℓ for leptons and q for nucleons (when several indices of the same species will be needed, we will add primes on the label as e.g. q, q'', q', etc.). We will apply the Einstein summation convention (i.e. repeated indices are summed) for space–time indices but not for the constituent labels.

Let us consider an arbitrary number of fluids that are interacting with each other. We follow the variational formalism developed by Carter (1989), which has been recently reviewed by Gourgoulhon (2006) and Andersson & Comer (2007). In this approach, the basic fluid variables are the particle four-currents n_{X}^{μ} of each fluid. The equation governing the dynamical evolution of each fluid is obtained from an action principle by considering variations of the fluid particle trajectories. Given a so-called master function Λ, which is the Lagrangian density of the system, and a set of four-force densities f_{ν}^{X} acting on each fluid, the hydrodynamic equations take the very simple form

$$n_{\mathrm{X}}^{\mu}\varpi_{\mu\nu}^{\mathrm{X}} + \pi_{\nu}^{\mathrm{X}}\nabla_{\mu}n_{\mathrm{X}}^{\mu} = f_{\nu}^{\mathrm{X}}\,, \tag{1}$$

where the vorticity two-form $\varpi_{\mu\nu}^{\mathrm{X}}$ is defined as the exterior derivative of the four-momentum covector

$$\pi_{\mu}^{\mathrm{X}} = \frac{\partial\Lambda}{\partial n_{\mathrm{X}}^{\mu}}, \tag{2}$$

namely

$$\varpi_{\mu\nu}^{\mathrm{X}} = 2\nabla_{[\mu}\pi_{\nu]}^{\mathrm{X}} = \nabla_{\mu}\pi_{\nu}^{\mathrm{X}} - \nabla_{\nu}\pi_{\mu}^{\mathrm{X}}. \tag{3}$$

It is understood that the partial derivative in equation (2) is taken with all other four-currents being kept constant. For a strict application of the variational principle, the forces should separately vanish $f_{\nu}^{\mathrm{X}} = 0$, which entails by contracting equation (1) with the corresponding four-current n_{X}^{ν}, that $\nabla_{\mu}n_{\mathrm{X}}^{\mu} = 0$. In this case, equation (1) therefore reduces to

$$n_{\mathrm{X}}^{\mu}\varpi_{\mu\nu}^{\mathrm{X}} = 0. \tag{4}$$

Note that despite the vanishing of the individual forces f_{ν}^{X}, the fluids are not independent of each other in general and the set of equation (4) is therefore not simply Euler equations. The couplings between the various fluids are hindered in the momenta π_{μ}^{X}.

The stress-energy tensor of the fluids can be expressed as

$$T_{\nu}^{\mu} = \Psi\,\delta_{\nu}^{\mu} + \sum_{\mathrm{X}} n_{\mathrm{X}}^{\mu}\pi_{\nu}^{\mathrm{X}}, \tag{5}$$

where Ψ can be interpreted as a generalized pressure and is defined by

$$\Psi = \Lambda - \sum_{\mathrm{X}} n_{\mathrm{X}}^{\mu}\pi_{\mu}^{\mathrm{X}}. \tag{6}$$

Let us emphasize that so far we have made no assumption with respect to the space–time geometry so that the above covariant expressions, based only on the exterior calculus, are valid both in (special and general) relativity and in the Newtonian limit. In the following sections, we will show how to construct the Lagrangian density Λ in each case.

3 NON-RELATIVISTIC TWO-FLUID MODELS OF NEUTRON STAR CORE

We consider a uniform mixture with four constituents: neutrons, protons, electrons and possibly muons. Such a composition is expected to be found in the interior of low-mass neutron stars and in the outer core of massive neutron stars at densities above the crust-core transition density $\rho_{\mathrm{cc}} \sim \rho_0/2$ and below $\lesssim 2$–$3\rho_0$, where $\rho_0 \simeq 2.8 \times 10^{14}\ \mathrm{g\,cm^{-3}}$ is the saturation density of infinite symmetric nuclear matter. Given the current uncertainties on the composition of neutron star core (for a recent review see e.g. Haensel et al. 2006), it is sometimes assumed for simplicity that this composition remains the same at higher densities.

At densities below $\sim 3\rho_0$, the nucleons are essentially non-relativistic. For instance, the sound velocity for the realistic model $A18 + \delta v + \mathrm{UIX}^*$ of Akmal, Pandharipande & Ravenhall (1998) becomes comparable to the speed of light at densities around $\sim 5\rho_0$. For this model, such densities are reached in very massive neutron stars with a mass larger than $2\,\mathrm{M}_{\odot}$. However, the most precisely measured neutron star masses (in neutron star binaries) lie below $1.5\,\mathrm{M}_{\odot}$ (Lattimer & Prakash 2007). Besides, as shown by Glendenning (2000) (chapter 3, section 4), the effects of General relativity are negligible at the microscopic scale. Moreover, at

the macrocoscopic scale, the fluid velocities are small compared to the speed of light. Indeed, the velocity at the equator of the most rapidly spinning neutron stars is only about ∼20 per cent of the speed of light (taking 1 ms for the period and 10 km for the radius). For the purpose of matching the microscopic nuclear model to the macroscopic hydrodynamical model, it will therefore be convenient to start with a local analysis considering non-relativistic fluids in the Newtonian framework. Such non-relativistic models can also be very useful by themselves for studying qualitatively the dynamics of superfluid mixtures in neutron stars (Andersson & Comer 2001). In order to facilitate the correspondence between relativistic and non-relativistic models, we will use the fully 4D covariant formalism developed by Carter & Chamel (2004, 2005a,b). We will then show how to construct fully relativistic fluid models in Section 4 (as required for a General relativistic description of the star). For simplicity, we only consider the possible presence of the magnetic field by supposing that leptons and protons are comoving, as discussed in Section 1. We therefore consider only two independent fluids: the neutron superfluid and the fluid of charged particles (protons, electrons and possibly muons). This two-fluid model includes the limit of non-superfluid neutron star cores since in this case all the particles are essentially comoving and can thus be treated as a single fluid (Baym et al. 1969). Including the magnetic field is in principle straightforward. It has been recently shown that under some circumstances the magnetic field can even be variationally taken into account in the purely Newtonian context despite the non-Galilean invariance of Maxwell's equations (Carter et al. 2006a). However, taking into account the magnetic field as a dynamical field implies a better understanding of the lepton dynamics as well as the proton superconductivity which is beyond the scope of the present model.

Let us now briefly review the 4D geometric structure of the Newtonian space–time (see Carter & Chamel 2004 for a detailed discussion). Newtonian theory postulates the existence of a universal time t, leading to a foliation of the space–time into 3D hypersurfaces. Each of these spatial sections are flat and are endowed with the 3D Euclidean metric, giving rise to the symmetric contravariant tensors $\eta^{\mu\nu}$ and $\eta_{\mu\nu}$ by pushforward and by pull-back, respectively. These tensors are not metric tensors since they are degenerate

$$\eta^{\mu\nu}t_\nu = 0, \qquad \eta_{\mu\nu}e^\nu = 0 \tag{7}$$

where $t_\nu = \partial_\nu t$ and the 'ether' flow vector e^μ, normalized by the condition

$$e^\mu t_\mu = 1, \tag{8}$$

characterizes a particular Aristotelian frame corresponding to the usual kind of 3+1 space–time decomposition. The particle four-currents introduced in Section 2 are given by $n_{\rm x}^\mu = n_{\rm x}u_{\rm x}^\mu$, where $n_{\rm x}$ are the corresponding particle number densities, and the four-velocities $u_{\rm x}^\mu$ are defined by

$$u_{\rm x}^\mu = v_{\rm x}^\mu + e^\mu, \qquad t_\mu v_{\rm x}^\mu = 0, \tag{9}$$

with $v_{\rm x}^\mu$ being the corresponding push forward of the usual three-velocities in the given Aristotelian frame. It is easily seen from equation (8) that the four-velocities are normalized as

$$t_\mu u_{\rm x}^\mu = 1. \tag{10}$$

We will neglect the small mass difference between neutrons and protons and write simply m for the nucleon mass, which we take to be equal to the atomic mass unit. For consistency, we thus take the electron mass $m^{\rm e} = 0$. We also neglect the muon mass except at the microscopic scale for calculating the internal energy density.

In the limit of small currents, the Lagrangian density Λ can be decomposed into a dynamical part $\Lambda_{\rm dyn}$, which depends on the particle currents $n_{\rm x}^\mu$, and a static part $\Lambda_{\rm ins}$ which depends only on the particle densities given by

$$n_{\rm x} = n_{\rm x}^\mu t_\mu. \tag{11}$$

The dynamical Lagrangian density (neglecting the contribution of the leptons) can be written as a quadratic form of the nucleon currents

$$\Lambda_{\rm dyn} = \frac{1}{2}\sum_{q,q'} \eta_{\mu\nu}\,\mathcal{K}^{qq'} n_q^\mu n_{q'}^\nu. \tag{12}$$

The coefficients of the symmetric mobility matrix $\mathcal{K}^{qq'}(q, q' = n, p$ for neutrons, protons, respectively) are functions of the nucleon densities and will be evaluated in Section 8. Due to the Galilean invariance, the matrix elements are related to each other by

$$\sum_{q'} n_{q'}\mathcal{K}^{qq'} = m. \tag{13}$$

Taking the partial derivative of the above equation with respect to the nucleon density leads to the following identity:

$$\sum_{q',q''} n_{q'}\frac{\partial \mathcal{K}^{q'q''}}{\partial n_q} n_{q''} = -m. \tag{14}$$

Since the left-hand side of equation (14) has to be negative for any neutron and proton densities, we obtain the following inequalities

$$\frac{\partial \mathcal{K}^{qq}}{\partial n_{q'}} < 0, \qquad \left(\frac{\partial \mathcal{K}^{np}}{\partial n_q}\right)^2 < \frac{\partial \mathcal{K}^{nn}}{\partial n_q}\frac{\partial \mathcal{K}^{pp}}{\partial n_q}. \tag{15}$$

The non-diagonal coefficient $\mathcal{K}^{np} = \mathcal{K}^{pn}$ accounts for the non-dissipative entrainment effects and arises from the strong interactions between nucleons. If the nucleons could be treated as ideal Fermi gases, this coefficient would simply vanish $\mathcal{K}^{np} = 0$.

The static contribution $\Lambda_{\rm ins}$ is related to the static internal (non-gravitational) energy density $U_{\rm ins}$ by

$$\Lambda_{\rm ins} = -U_{\rm ins} - U_{\rm pot}, \tag{16}$$

where ρ is the total baryon mass density

$$\rho = m n_{\rm b} \tag{17}$$

and $U_{\rm pot} = \rho\phi$ is the gravitational potential energy density, ϕ being the gravitational scalar potential. As discussed previously, nucleons are not relativistic either at the microscopic scale or at the macroscopic scale. Nevertheless, in order to prepare the generalization to relativistic fluids in the next section, the nucleon rest-mass energy density is included in $U_{\rm ins}$. It can be shown that in the Newtonian framework this extra term has no effect on the variational principle (thereby on the dynamical equations of the fluids) provided the total mass current is conserved (Carter et al. 2006a). Let us point out that the total internal (non-gravitational) energy density $U_{\rm int}$ is not simply given by $U_{\rm ins}$, but contains an additional entrainment term defined by $U_{\rm ent} = U_{\rm dyn} - U_{\rm kin}$, where $U_{\rm dyn} = \Lambda_{\rm dyn}$ and

$$U_{\rm kin} = \frac{1}{2}\sum_q \eta_{\mu\nu}\frac{m}{n_q} n_q^\mu n_q^\nu \tag{18}$$

is the total kinetic energy density. We thus have $U_{\rm int} = U_{\rm ins} + U_{\rm ent}$.

In summary, the non-relativistic Lagrangian density of the fluids is therefore given by

$$\Lambda = \Lambda_{\rm dyn} + \Lambda_{\rm ins}, \tag{19}$$

where $\Lambda_{\rm dyn}$ and $\Lambda_{\rm ins}$ are given by equations (12) and (16), respectively. The dynamical equations of the gravitational field can be

obtained from the variational principle by simply adding the contribution

$$\Lambda_{\rm grf} = -\frac{1}{8\pi G}\eta^{\mu\nu}(\nabla_\mu\phi)(\nabla_\nu\phi), \tag{20}$$

where G is the gravitational constant. Considering variations of the *total* Lagrangian density $\Lambda_{\rm tot} = \Lambda + \Lambda_{\rm grf}$ with respect to ϕ leads to the usual Poisson's equation

$$\eta^{\mu\nu}\nabla_\mu\nabla_\nu\phi = 4\pi G\rho. \tag{21}$$

Given the above Lagrangian density (19), the momentum of each constituent is obtained from equation (2). The nucleon momentum is given by

$$\pi^q_\mu = \sum_{q'}\eta_{\mu\nu}\,\mathcal{K}^{qq'}n^\nu_{q'} + t_\mu\left(\frac{1}{2}\sum_{q',q''}\eta_{\rho\nu}\frac{\partial\mathcal{K}^{q'q''}}{\partial n_q}n^\rho_{q'}n^\nu_{q''} - \mu_q - m\phi\right), \tag{22}$$

where $\mu_{\rm x}$ is the chemical potential defined by

$$\mu_{\rm x} = \frac{\partial U_{\rm ins}}{\partial n_{\rm x}}. \tag{23}$$

Since the Lagrangian density depends only on the lepton densities $n_\ell = n^\mu_\ell t_\mu (\ell = e, \mu$ for electrons, muons, respectively), the momenta of the leptons are time-like and are given by

$$\pi^\ell_\mu = -t_\mu\mu_\ell. \tag{24}$$

If the particles are all comoving with the four-velocity u^μ, the nucleon four-momenta take the familiar expression

$$\pi^q_\mu = m\eta_{\mu\nu}u^\nu - t_\mu\left(\frac{1}{2}mv^2 + \mu_q + m\phi\right), \tag{25}$$

where $v^2 = \eta_{\mu\nu}u^\nu u^\mu$, using the identities (13) and (14).

The usual three-momentum covector, denoted by $\Pi^{\rm x}_\mu$, is defined by the Aristotelian spatial components of the four-momentum covector $\pi^{\rm x}_\mu$,

$$\Pi^{\rm x}_\mu = \eta^\nu_\mu\pi^{\rm x}_\nu, \tag{26}$$

where η^μ_ν is the space projection tensor defined by

$$\eta^\mu_\nu = \delta^\mu_\nu - e^\mu t_\nu, \tag{27}$$

using the Kronecker unit tensor δ^μ_ν. It follows immediately from equation (8) that $e^\mu\Pi^{\rm x}_\mu = 0$. It is readily seen that the lepton three-momentum vanishes $\Pi^\ell_\mu = 0$, while the nucleon three-momentum is determined solely by the mobility matrix $\mathcal{K}^{qq'}$

$$\Pi^q_\nu = \sum_{q'}\eta_{\nu\mu}\,\mathcal{K}^{qq'}n^\mu_{q'}. \tag{28}$$

From the nucleon and lepton momenta equations (22) and (24), respectively, we can obtain the generalized pressure Ψ of the fluids according to equation (6). The kinetic part of the Lagrangian density $\Lambda_{\rm kin} = U_{\rm kin}$ does not contribute to the pressure Ψ which can thus be written as

$$\Psi = \Lambda_{\rm int} - \sum_{\rm x} n^\mu_{\rm x}\frac{\partial\Lambda_{\rm int}}{\partial n^\mu_{\rm x}}, \tag{29}$$

where $\Lambda_{\rm int} = \Lambda - \Lambda_{\rm kin}$. Due to entrainment effects, this internal Lagrangian density $\Lambda_{\rm int}$ of the fluids is not simply equal to the opposite of the *total* internal energy density (including gravitational contribution) $U_{\rm int} + U_{\rm pot}$ but is given by

$$\Lambda_{\rm int} = -U_{\rm int} - U_{\rm pot} + 2U_{\rm ent}. \tag{30}$$

The gravitational potential energy density does not contribute to the pressure. As a result, the generalized pressure Ψ is the sum of a static term $\Psi_{\rm ins}$ given by

$$\Psi_{\rm ins} = \sum_{\rm x} n_{\rm x}\frac{\partial U_{\rm ins}}{\partial n_{\rm x}} - U_{\rm ins}, \tag{31}$$

and a dynamical term is given by

$$\Psi_{\rm ent} = -\sum_{\rm x} n^\mu_{\rm x}\frac{\partial U_{\rm ent}}{\partial n^\mu_{\rm x}} + U_{\rm ent}. \tag{32}$$

In the single fluid case, the static pressure $\Psi_{\rm ins}$ reduces to the ordinary pressure usually denoted by P. Note that in multifluid systems, if the static internal energy density is of the form

$$U_{\rm ins} = \sum_{\rm x} U^{\rm x}\{n_{\rm x}\}, \tag{33}$$

the static pressure can then be written as the sum of the partial pressures $P_{\rm x}$

$$P = \sum_{\rm x} P_{\rm x} \tag{34}$$

with

$$P_{\rm x} = \sum_{\rm x} n_{\rm x}\frac{\partial U^{\rm x}}{\partial n_{\rm x}} - U^{\rm x}. \tag{35}$$

In the general case, however, such a decomposition is not possible. The additional pressure term $\Psi_{\rm ent}$ vanishes whenever either the two fluids are comoving or the fluids are non-interacting so that the non-diagonal coefficients of the mobility matrix vanish (no entrainment).

Going back to the two-fluid model of neutron star cores, the static and entrainment contributions to the general pressure are given explicitly by

$$\Psi_{\rm ins} = n_{\rm n}\frac{\partial U_{\rm ins}}{\partial n_{\rm n}} + n_p\frac{\partial U_{\rm ins}}{\partial n_p} + n_e\frac{\partial U_{\rm ins}}{\partial n_e} + n_\mu\frac{\partial U_{\rm ins}}{\partial n_\mu} - U_{\rm ins} \tag{36}$$

and

$$\Psi_{\rm ent} = \frac{1}{2}\eta_{\mu\nu}\left(v^\mu_p - v^\mu_{\rm n}\right)\left(v^\nu_p - v^\nu_{\rm n}\right) \times\left[n^2_{\rm n}\frac{\partial m^n_\star}{\partial n_{\rm n}} + n^2_p\frac{\partial m^p_\star}{\partial n_p} + \frac{1}{2}n_{\rm n}(m^n_\star - m) + \frac{1}{2}n_p(m^p_\star - m)\right], \tag{37}$$

respectively. Given the general pressure $\Psi = \Psi_{\rm ent} + \Psi_{\rm ins}$ and the four-momenta $\pi^{\rm x}_\mu$ of the various constituents, the stress-energy tensor of the fluids can easily be obtained from equation (5).

4 FROM NON-RELATIVISTIC TO RELATIVISTIC TWO-FLUID MODELS

In the previous section, we have taken into account of the effects of the gravitational field on the fluids by including the term $-\rho\phi$ in the static internal Lagrangian density $\Lambda_{\rm ins}$. Alternatively, as was first shown by Elie Cartan, the effects of gravitation can be taken into account in the structure of the Newtonian space–time itself, thus facilitating the comparison with General relativity (see e.g. chapter 12 of Misner, Thorne & Wheeler 1973). This can be achieved by replacing the tensor $\eta_{\mu\nu}$ in equation (12) for the Newton–Cartan space–time metric $\gamma_{\mu\nu}$ defined by

$$\gamma_{\mu\nu} = \eta_{\mu\nu} - 2\phi t_\mu t_\nu. \tag{38}$$

It is readily verified, remembering equation (13), that this is indeed completely equivalent to adding the term $-\rho\phi$ to the Lagrangian

density Λ. However, using this approach, it becomes clear how to make the correspondence with General relativity (thereby Special relativity as well). For weak gravitational fields, the Riemannian metric $g_{\mu\nu}$ of the relativistic space–time can be locally approximated by

$$g_{\mu\nu} \simeq \eta_{\mu\nu} - (c^2 + 2\phi)t_\mu t_\nu = \gamma_{\mu\nu} - c^2 t_\mu t_\nu. \tag{39}$$

This suggests to define the 'dynamical' contribution to the relativistic Lagrangian density as

$$\widetilde{\Lambda}_{\rm dyn} = \frac{1}{2}\sum_{q,q'} \mathcal{K}^{qq'}\,\left(g_{\mu\nu} n_q^\mu n_{q'}^\nu + c^2 n_q n_{q'}\right), \tag{40}$$

where $n_q^\mu = n_q u_q^\mu$. The particle densities $n_{\rm x}$ are now defined by

$$n_{\rm x} = \sqrt{-g_{\mu\nu} n_{\rm x}^\mu n_{\rm x}^\nu}/c, \tag{41}$$

with the four-velocities normalized as

$$g_{\mu\nu} u_{\rm x}^\mu u_{\rm x}^\nu = -c^2. \tag{42}$$

Note that equation (41) with the normalization (42) is consistent with equations (9) and (10) in the non-relativistic limit. Likewise, with the definition (40), the expression (12) is indeed recovered in the Newtonian limit.

The relativistic expression of the corresponding 'static' part is readily obtained by simply substituting the particle densities of the constituents in the Newtonian ether frame for the densities (41) in the rest frame of the corresponding particles. Using the identity (13) and adding the internal energy density, the total relativistic Lagrangian density of the fluids can be expressed as

$$\widetilde{\Lambda} = \frac{1}{2}\sum_{q,q'} \mathcal{K}^{qq'}\, g_{\mu\nu} n_q^\mu n_{q'}^\nu + \frac{1}{2} n_{\rm b} m c^2 - U_{\rm ins}, \tag{43}$$

where $n_{\rm b} = n_{\rm n} + n_p$ is the baryon density. If the fluids are described in General relativity, the Lagrangian (43) has to be complemented with the Einstein–Hilbert contribution

$$\widetilde{\Lambda}_{\rm grf} = \frac{c^4}{16\pi G} R, \tag{44}$$

where R is the Ricci scalar associated with the metric $g_{\mu\nu}$. Variations of the action with respect to the metric (which involve not only variations of the total Lagrangian density but also variations of the space–time measure) lead to Einstein's equations (see e.g. Andersson & Comer 2007).

The relativistic momenta of the nucleons can be expressed in a form similar to equation (26) as

$$\pi_\mu^q = \sum_{q'} g_{\mu\nu} \widetilde{\mathcal{K}}^{qq'} n_{q'}^\nu. \tag{45}$$

The non-diagonal components of the symmetric relativistic mobility matrix $\widetilde{\mathcal{K}}^{qq'}$ are equal to those of the non-relativistic matrix $\mathcal{K}^{qq'}$, while the diagonal elements are given by

$$\widetilde{\mathcal{K}}^{qq} = \mathcal{K}^{qq} - \frac{m}{n_q} + \frac{\mu_q}{c^2 n_q} - \frac{1}{c^2 n_q}\frac{\partial \mathcal{K}^{np}}{\partial n_q}\left(c^2 n_{\rm n} n_p + g_{\rho\sigma} n_{\rm n}^\rho n_p^\sigma\right). \tag{46}$$

The relativistic momenta of the leptons take a very simple form

$$\pi_\nu^\ell = \frac{\mu_\ell}{c^2} u_p^\mu\, g_{\mu\nu}. \tag{47}$$

If the constituents are all comoving with the four-velocity u^μ, the four-momenta reduce to

$$\pi_\nu^{\rm x} = \frac{\mu_{\rm x}}{c^2} u^\mu\, g_{\mu\nu}. \tag{48}$$

With the momenta specified, we can obtain the generalized pressure Ψ from equation (6). As for the non-relativistic case, Ψ can be decomposed into an ordinary 'static' part given by equation (31) and an extra contribution $\Psi_{\rm ent}$ due to entrainment which can be expressed as

$$\Psi_{\rm ent} = -\sum_{\rm x} n_{\rm x}^\mu \frac{\partial \widetilde{U}_{\rm ent}}{\partial n_{\rm x}^\mu} + \widetilde{U}_{\rm ent}, \tag{49}$$

where the entrainment energy density is now defined by

$$\widetilde{U}_{\rm ent} = \frac{1}{2}\sum_{q,q'} \mathcal{K}^{qq'}\, g_{\mu\nu} n_q^\mu n_{q'}^\nu. \tag{50}$$

Before concluding this section, let us remark that the relativistic Lagrangian density can be written in the very concise form

$$\widetilde{\Lambda} = \lambda_0 + \lambda_1 (x^2 - np), \tag{51}$$

where the coefficients λ_0 and λ_1 are given by

$$\lambda_0 = -U_{\rm ins}, \qquad \lambda_1 = -c^2 \mathcal{K}^{np}, \tag{52}$$

and adopting the following notations

$$x^2 c^2 = -g_{\mu\nu} n_{\rm n}^\mu n_p^\nu, \tag{53}$$

$$n^2 c^2 = -g_{\mu\nu} n_{\rm n}^\mu n_{\rm n}^\nu, \tag{54}$$

$$p^2 c^2 = -g_{\mu\nu} n_p^\mu n_p^\nu. \tag{55}$$

Equation (51) is consistent with the expansion of the Lagrangian density in powers of $(x^2 - np)$, suggested by Andersson et al. (2002). It can be clearly seen in equation (51) that in the absence of entrainment (i.e. $\lambda_1 = 0$) or in the case of comoving fluids, the Lagrangian density reduces to the opposite of the internal energy density.

5 DYNAMICAL EFFECTIVE MASSES

5.1 Non-relativistic case

If the nucleons were not interacting with each other, the mobility matrix introduced in Section 3 would be diagonal and we would simply have $\mathcal{K}^{nn} = m/n_{\rm n}$ and $\mathcal{K}^{pp} = m/n_p$. Of course, we know that nucleons are strongly interacting. This means that the matrix $\mathcal{K}^{qq'}$ does not have such a simple structure. It is convenient to define neutron and proton dynamical effective masses by

$$m_\star^n \equiv n_{\rm n}\,\mathcal{K}^{nn}, \quad m_\star^p \equiv n_p\,\mathcal{K}^{pp}, \tag{56}$$

respectively. The deviations of $m_\star^q$ from the bare baryon mass m therefore arise entirely from the nucleon–nucleon interactions. Let us point out that these effective masses depend on the nucleon densities and therefore vary with depth inside the neutron star. As a result of equation (13), the non-diagonal coefficients of the mobility matrix can be expressed as

$$\mathcal{K}^{np} = \mathcal{K}^{pn} = \frac{m - m_\star^n}{n_p} = \frac{m - m_\star^p}{n_{\rm n}}. \tag{57}$$

It can be shown with stability arguments (Chamel & Haensel 2006) that the effective masses are bounded from below $m_\star^q/m > n_q/n_{\rm b}$, where $n_{\rm b} = n_{\rm n} + n_p$ or equivalently

$$\mathcal{K}^{np} = \mathcal{K}^{pn} < \frac{m}{n_{\rm b}}. \tag{58}$$

Since in neutron star core the effective masses are typically *smaller* than the bare nucleon mass (therefore $\mathcal{K}^{np} > 0$), this inequality

provides an upper bound for the largest possible strength of entrainment effects between the two fluids. The physical meaning of the dynamical effective masses defined by equation (56) becomes clear when writing the expressions of the nucleon three-momentum covectors (26)

$$\Pi^n_\nu = m^n_\star v_{\mathrm{n}\,\nu} + (m - m^n_\star) v_{p\,\nu}, \tag{59}$$

$$\Pi^p_\nu = m^p_\star v_{p\,\nu} + (m - m^p_\star) v_{\mathrm{n}\,\nu}, \tag{60}$$

where $v_{\mathrm{x}\,\nu} \equiv \eta_{\nu\mu} v^\mu_{\mathrm{x}}$. This shows that the three-momentum and the three-velocity of a given nucleon species are not aligned whenever the dynamical effective masses differ from the bare nucleon mass, or equivalently whenever the non-diagonal coefficients of the mobility matrix do not vanish.

5.2 Relativistic case

By analogy with the definition (56), let us introduce relativistic nucleon dynamical effective masses by

$$\widetilde{m}^q_\star = n_q \widetilde{\mathcal{K}}^{qq}, \tag{61}$$

where $\widetilde{\mathcal{K}}^{qq'}$ is the relativistic generalization of the non-relativistic mobility matrix $\mathcal{K}^{qq'}$. Using equation (46) together with (56), we find

$$\frac{\widetilde{m}^q_\star}{m} = \frac{m^q_\star}{m} + \frac{\mu_q}{mc^2} - 1 - \frac{1}{mc^2}\frac{\partial \mathcal{K}^{np}}{\partial n_q}\left(c^2 n_{\mathrm{n}} n_p + g_{\rho\sigma} n^\rho_{\mathrm{n}} n^\sigma_p\right), \tag{62}$$

with μ_q the chemical potential defined by equation (23). It is easily checked that $\widetilde{m}^q_\star \to m^q_\star$ in the Newtonian limit. With these definitions, the neutron and proton four-momenta can be explicitly written as

$$\pi^n_\mu = \left[\widetilde{m}^n_\star u^\nu_{\mathrm{n}} + (m - m^n_\star) u^\nu_p\right] g_{\mu\nu}, \tag{63}$$

$$\pi^p_\mu = \left[\widetilde{m}^p_\star u^\nu_p + (m - m^p_\star) u^\nu_{\mathrm{n}}\right] g_{\mu\nu}. \tag{64}$$

Note that the entrainment contributions involve the *non-relativistic* effective masses (56). Equation (62) is the generalization to interacting multifluid systems of the effective mass introduced by Carter (1989) in the perfect fluid case. Indeed, in the absence of entrainment, $\mathcal{K}^{np} = 0$ so that $m^q_\star = m$ while the relativistic effective masses are given by

$$\frac{\widetilde{m}^q_\star}{m} = \frac{\mu_q}{mc^2}. \tag{65}$$

This equation is identical to equation (1.66) in the lecture notes of Carter (1989). The physical origin of the difference between $\widetilde{m}^q_\star$ and $m^q_\star$ is that in relativity *all* forms of energy contribute to the mass. A remarkable consequence is that even massless particles can have a non-vanishing relativistic effective mass. This is for instance the case of leptons for which we have assumed $m^\ell = 0$. However, equation (47) shows that the dynamical effective lepton mass is not zero but is given by

$$\widetilde{m}^\ell_\star = \frac{\mu_\ell}{c^2}. \tag{66}$$

Note that even if leptons were not interacting (which we will actually suppose in Section 8 in order to evaluate the master function Λ), they would still have a non-zero effective mass due to the Pauli exclusion principle which prevents all the particles from occupying the lowest energy state with zero momentum (the chemical potential μ_ℓ is then given by the Fermi energy of the lepton species ℓ).

For unbound nuclear systems like the liquid core of neutron stars, we have $\mu_q > mc^2$. Besides, if we assume that the strength of entrainment effects decreases with increasing density, i.e.

$$\frac{\partial \mathcal{K}^{np}}{\partial n_q} < 0, \tag{67}$$

(this is actually the case for the models considered in this work; see equation 109), and using the Cauchy–Schwartz inequality

$$-g_{\mu\nu} n^\mu_{\mathrm{n}} n^\nu_p \le \sqrt{-g_{\mu\nu} n^\mu_{\mathrm{n}} n^\nu_{\mathrm{n}}}\sqrt{-g_{\mu\nu} n^\mu_p n^\nu_p}, \tag{68}$$

it is easily shown that the relativistic effective masses are always larger than the non-relativistic ones. With the notations introduced at the end of Section 4, the relativistic dynamical effective masses can be expressed solely in terms of the parameters λ_0 and λ_1 of the relativistic Lagrangian density as

$$\widetilde{m}^q_\star = (n_{\mathrm{b}} - n_q)\frac{\lambda_1}{c^2} - \frac{1}{c^2}\frac{\partial \lambda_0}{\partial n_q} + \frac{1}{c^2}\frac{\partial \lambda_1}{\partial n_q}(np - x^2). \tag{69}$$

Note that the first-order expansion of the relativistic Lagrangian density, equation (51) in powers of $(x^2 - np)$, leads to dynamical effective masses with a first-order contribution proportional to $(x^2 - np)$. This velocity-dependent term vanishes in the Newtonian limit so that the non-relativistic effective masses are independent of the velocities to the first order. The reason is that in relativity the particle number densities involve all the components of the corresponding four-currents according to equation (41) while in the Newtonian case, the densities only depend on the time component of the four-current through equation (11).

6 SUPERFLUIDITY

In the previous sections, we have accounted for the superfluidity in neutron star core by assuming that two independent fluid motions could coexist. However, strictly speaking this assumption only requires perfect fluidity, i.e. the absence of viscosity and dissipative drag effects which damp the development of relative motions between the constituents. The distinguishing feature of a superfluid compared to a perfect fluid is the fact that it can be described by a macroscopic quantum wave function. This entails that in a superfluid the momentum circulation is quantized according to the Bohr–Sommerfeld quantization rule

$$\oint \pi_\mu \mathrm{d}x^\mu = N\pi\hbar, \tag{70}$$

where $\hbar$ is the Dirac–Planck constant and N is an integer, which simply follows from the requirement that the length of any closed path must be an integral multiple of the de Broglie wavelength of the condensate formed of bound neutron pairs. This condition implies the existence of neutron quantized vortex lines in neutron stars (Ginzburg & Kirzhnits 1965). Assuming that the neutron vortices are arranged on a regular triangular array, the inter vortex spacing is given by

$$d_\upsilon = \sqrt{\frac{h}{2\sqrt{3} m \Omega_{\mathrm{n}}}} \simeq 3.4 \times 10^{-3}\sqrt{\frac{10^2\ \mathrm{s}^{-1}}{\Omega}}\ \mathrm{cm}, \tag{71}$$

where Ω_{n} is the angular velocity of the neutron superfluid, which is approximately equal to the observed angular velocity Ω of the star.

In regions devoid of vortices, the neutron momentum circulation is equal to zero which implies that the neutron momentum can be written as

$$\pi^n_\mu = \frac{\hbar}{2}\nabla_\mu \varphi^n, \tag{72}$$

where the factor of 1/2 accounts for the fermionic nature of the neutrons and φ^n is the scalar phase of the condensate. Consequently, the corresponding vorticity two-form *locally* vanishes

$$\varpi^n_{\mu\nu} = 0. \tag{73}$$

However, at length-scales much larger than d_υ for which we are interested here, a fluid element is threaded by many vortex lines. Consequently, the vorticity two-form does not have to vanish at this scale. Nevertheless, the superfluidity condition requires the existence of an average four-velocity vector u^μ_υ of the vortex lines such that the Lie derivative of the vorticity two-form along u^μ_υ vanishes

$$\boldsymbol{u}_\upsilon \mathcal{L} \varpi^n_{\mu\nu} = 0. \tag{74}$$

The above condition is satisfied if

$$u^\mu_\upsilon \varpi^n_{\mu\nu} = 0. \tag{75}$$

Vortices are comoving with the superfluid, unless forces act on them. Indeed, it can be seen that equation (75) with $u^\mu_\upsilon = u^\mu_{\rm n}$ is consistent with Euler equation (4) obtained for the case $f^n{}_\nu = 0$. It should be stressed that the above conditions (73) and (75) apply for either relativistic or non-relativistic superfluid. The presence of vortices can be explicitly included in the variational principle as shown by Carter (2000) and will not be further discussed here.

7 COMPOSITION OF NEUTRON STAR CORE

The composition of the neutron star core is determined by the rates of transfusion processes which convert particles of different species into each other. While the baryon number is always conserved

$$\nabla_\mu n^\mu_b = 0, \tag{76}$$

where $n^\mu_{\rm b} = n^\mu_{\rm n} + n^\mu_p$, neutrons may be transformed into protons and vice versa via electroweak processes. The fastest process is the direct Urca process

$$n \to p^+ + \ell + \bar{\nu}_\ell, \quad p^+ + \ell \to n + \nu_\ell, \tag{77}$$

where ℓ is electron or muon. When the beta equilibrium is reached, the two reactions occur at the same rate. In degenerate dense matter, this process is allowed for sufficiently large proton fractions owing to the requirement that both momentum and energy have to be conserved (Lattimer et al. 1991). When these reactions are forbidden, the slower modified Urca process prevails

$$n + N \to p^+ + \ell + \bar{\nu}_\ell, \quad p^+ + N + \ell \to n + \nu_\ell, \tag{78}$$

involving an additional spectator nucleon N (neutron or proton). The relaxation time of these beta processes for *npe* matter, neglecting nucleon superfluidity, is approximately given by $\tau^{(D)} \sim 20 T_9^{-4}$ s and $\tau^{(M)} \sim T_9^{-6}$ months for the direct and modified Urca processes, respectively, where T_9 is the temperature in units of 10^9 K (Yakovlev et al. 2001). Electrons and muons are transformed into each other via the lepton-modified Urca processes

$$e^- + X \to \mu^- + X + \bar{\nu}_\mu + \nu_e, \quad \mu^- + X \to e^- + X + \bar{\nu}_e + \nu_\mu, \tag{79}$$

where X is either a nucleon or a lepton (the direct process is kinematically forbidden). The relaxation time associated with electromagnetic processes, of the order of 10^{-22} s (Easson & Pethick 1979), is much smaller than the characteristic time-scales of the neutron star phenomena considered here, so that the matter can be treated as electrically neutral. This condition reads

$$n_p = n_e + n_\mu. \tag{80}$$

In the newly born proto–neutron stars, the temperatures are of the order of $\sim 10^{11}$ K or higher so that the equilibrium is reached in a few microseconds for the modified Urca process or 10 times less for the direct Urca. As the star cools down to temperatures $\sim 10^9$ K after 10^3– 10^4 yr, the relaxation times rise dramatically to about 20 s for the direct Urca and several months for the modified Urca. Besides, when the temperature falls below the critical threshold for the onset of superfluidity, the relaxation times increase exponentially (Villain & Haensel 2005). As a consequence, for the short time-scales of $\sim$1–100 milliseconds relevant for oscillations of mature neutron stars (like the recently observed QPOs in SGR), the composition of the star remains essentially frozen and the constituents can therefore be assumed to be separately conserved

$$\nabla_\mu n^\mu_p = 0, \quad \nabla_\mu n^\mu_e = 0, \tag{81}$$

which entails by equations (76) and (80), that the other currents are also conserved $\nabla_\mu n^\mu_{\rm n} = 0$ and $\nabla_\mu n^\mu_\mu = 0$ (remembering that the leptons are comoving with the protons). Let us remark that the lepton number is not conserved unlike the baryon number, because the neutron star matter is transparent to neutrinos (except for the first few seconds after its birth into a hot proto-neutron star).

The initial equilibrium composition of the neutron star core is obtained from the condition of electroneutrality (80) and the conditions that the chemical affinities corresponding to the above processes should vanish (Carter & Chamel 2005b). The chemical affinity $\mathcal{A}^\Xi$ of a given reaction Ξ is defined by (Carter & Chamel 2005b)

$$\mathcal{A}^\Xi = -\sum_{\rm X} N^\Xi_{\rm X} \mathcal{E}^{\rm X}, \tag{82}$$

where $N^\Xi_{\rm X}$ and $\mathcal{E}^{\rm X}$ are the relevant particle creation numbers and the energies per particle, respectively. As pointed out by Carter & Chamel (2005b), the problem arises of determining the reference frame with respect to which the energies $\mathcal{E}^{\rm X}$ have to be measured when some of the constituents (here neutrons and charged particles) are moving with different velocities. Since the relative velocity between the two fluids is expected to be small compared to the fluid velocities, we assume for simplicity in this section that the particles are all comoving with four-velocity u^μ. It is then natural to define the energy per particle as $\mathcal{E}^{\rm X} = -u^\mu \pi^{\rm X}_\mu$. In the Newtonian case, using equation (25) we thus have

$$\mathcal{E}^{\rm X} = \mu_{\rm X} + m^{\rm X}\phi - \frac{1}{2} m^{\rm X} v^2, \tag{83}$$

where the chemical potential of a particle species X is defined by equation (23). Since the mass is conserved in any chemical reaction Ξ involving *non-relativistic* particles, the corresponding chemical affinity (82) reduces to

$$\mathcal{A}^\Xi = -\sum_{\rm X} N^\Xi_{\rm X} \mu_{\rm X}. \tag{84}$$

In the relativistic case, the energy per particle obtained from equation (48) is given by

$$\mathcal{E}^{\rm X} = \mu_{\rm X}, \tag{85}$$

so that equation (84) is valid for both relativistic and non-relativistic particles.

We assume that neutrinos have escaped from the star so that we set $\mathcal{E}^{\nu_\ell} = 0$. Both the direct and modified Urca processes, respectively (77) and (78), have the same affinity given by

$$\mathcal{A}^{\rm Urca} = \mathcal{E}^n - \mathcal{E}^p - \mathcal{E}^e. \tag{86}$$

The electron–muon transfusion reactions (79) are characterized by the affinity

$$\mathcal{A}^{\mu e} = \mathcal{E}^e - \mathcal{E}^\mu. \tag{87}$$

The composition of the core at a given baryon density, $n_{\rm b}$, can then be determined by solving the equations $\mathcal{A}^{\rm Urca} = 0 = \mathcal{A}^{\mu e}$ under the constraint (80). Using (84), this leads to

$$\mu_{\rm n} = \mu_e + \mu_p, \tag{88}$$

$$\mu_e = \mu_\mu. \tag{89}$$

If the matter is in equilibrium, the static pressure depends only on the baryon density $n_{\rm b}$ and can be written in the concise form (valid in both the relativistic case and the Newtonian limit)

$$\Psi_{\rm ins} = n_{\rm b}\mu_{\rm n} - U_{\rm ins} \tag{90}$$

where $\mu_{\rm n}$ is the neutron chemical potential evaluated at the *equilibrium* neutron and proton densities, associated with the baryon density $n_{\rm b}$. Let us emphasize that equation (90) is only valid for neutron star matter in *equilibrium*. In the general case, the static pressure is given by equation (31).

8 EVALUATION OF THE MICROSCOPIC PARAMETERS

The internal static energy density can be decomposed into several contributions

$$U_{\rm ins}\left\{n_{\rm n}, n_p, n_e, n_\mu\right\} = U_{\rm N}\left\{n_{\rm n}, n_p\right\} + U_{\rm Coul}\left\{n_p, n_e, n_\mu\right\} + U_{\rm L}\left\{n_e\right\} + U_{\rm L}\left\{n_\mu\right\}, \tag{91}$$

where $U_{\rm N}$ is the nucleon part, $U_{\rm Coul}$ is the Coulomb part and $U_{\rm L}$ the lepton (kinetic) part. The Coulomb energy arises from lepton–lepton, lepton–proton and proton–proton interactions. It is of purely quantum origin since the classical contribution coming from Poisson's equation vanishes as a result of electroneutrality. We neglect the lepton–lepton interactions (but not the lepton–proton interactions) and we approximate the proton Coulomb energy by the Hartree–Fock exchange energy of non-relativistic point-like charged particles

$$U_{\rm Coul}\{n_p\} = -\frac{3}{4}e^2\left(\frac{3}{\pi}\right)^{1/3} n_p^{4/3}. \tag{92}$$

Unlike nucleons, leptons are relativistic at the microscopic scale (note however that this does not imply that their *collective* motion is relativistic at the *macroscopic* scale of the fluid description). Their kinetic energy is thus given by that of an ideal relativistic Fermi gas ($\ell = e, \mu$)

$$U_{\rm L}\left\{n_\ell\right\} = \frac{\hbar c}{8\pi^2\lambda_\ell^4}\left[x_\ell(2x_\ell^2+1)\sqrt{x_\ell^2+1} - \ln\left(x_\ell + \sqrt{x_\ell^2+1}\right)\right], \tag{93}$$

where $\lambda_\ell = \hbar/m_\ell c$ is the Compton wavelength and the dimensionless parameter x_ℓ is defined in terms of the Fermi wave number

$$k_{{\rm F}\ell} = (3\pi^2 n_\ell)^{1/3}, \tag{94}$$

by

$$x_\ell = \lambda_\ell k_{{\rm F}\ell}. \tag{95}$$

Since the electron mass is set to zero, the electron energy density is obtained by taking the limit $x_e \to +\infty$ of equation (93) yielding

$$U_{\rm L}\{n_e\} = \frac{p_{{\rm F}e}^4}{4\pi^2(\hbar c)^3}, \tag{96}$$

where $p_{{\rm F}e} = \hbar\, k_{{\rm F}e}$ is the electron Fermi momentum.

The strong interactions among nucleons are described by an effective Hamiltonian with a two-body force of the Skyrme type (Bender, Heenen & Reinhard 2003; Stone & Reinhard 2007)

$$v\{\boldsymbol{r}_1, \boldsymbol{r}_2\} = t_0(1+x_0P_\sigma)\delta\{\boldsymbol{r}\} + \frac{t_1}{2}(1+x_1P_\sigma)\left(\boldsymbol{k}'^2\delta\{\boldsymbol{r}\} + \delta\{\boldsymbol{r}\}\boldsymbol{k}^2\right) + t_2(1+x_2P_\sigma)\boldsymbol{k}'\cdot\delta\{\boldsymbol{r}\}\boldsymbol{k} \tag{97}$$

$$+ \frac{t_3}{6}(1+x_3P_\sigma)\delta\{\boldsymbol{r}\}n_{\rm b}\{\boldsymbol{R}\}^\alpha + {\rm i}W_0(\boldsymbol{\sigma}_1+\boldsymbol{\sigma}_2)\cdot\boldsymbol{k}'\times\delta\{\boldsymbol{r}\}\boldsymbol{k}, \tag{98}$$

where $\boldsymbol{r} = \boldsymbol{r}_1 - \boldsymbol{r}_2$, $\boldsymbol{R} = (\boldsymbol{r}_1 + \boldsymbol{r}_2)/2$, $\boldsymbol{\sigma}_1$ and $\boldsymbol{\sigma}_2$ are Pauli spin matrices, $\boldsymbol{k} = -{\rm i}(\nabla_1 - \nabla_2)/2$ is the relative wave vector, $\boldsymbol{k}'$ is the complex conjugate of $\boldsymbol{k}$ acting on the left and $P_\sigma = (1+\boldsymbol{\sigma}_1\cdot\boldsymbol{\sigma}_2)/2$ is the spin-exchange operator. The first term represents the attractive part of the nucleon–nucleon interaction. The next two momentum-dependent terms are associated with the finite range of the interaction. The density-dependent term proportional to t_3 corresponds to the strongly repulsive short-range part of the interaction and simulates the effects of three-body interactions (Vautherin & Brink 1972). The last term which leads to spin-orbit coupling in finite nuclei does not contribute in uniform matter. In principle, as shown by Negele & Vautherin (1972), this effective interaction can be derived from the 'bare' nucleon–nucleon interaction by expanding the nucleon density matrix in relative and centre of mass coordinates, $\boldsymbol{r}, \boldsymbol{R}$, respectively. In practice, however, the parameters are usually determined by fitting experimental data and/or results of microscopic many-body calculations in infinite uniform nuclear matter using the bare nucleon–nucleon interactions. Such kind of zero range effective forces are valid whenever the inter particle spacing is much larger than the range of the nuclear interactions. This condition is satisfied at densities below $\sim 3\rho_0$. Nevertheless, since these effective forces are usually constrained to reproduce the high-density equation of state of nuclear matter, it is not completely unreasonable to apply them at densities above $\sim 3\rho_0$. Finite range effects of the nucleon–nucleon interaction as well as relativistic corrections are somehow taken into account phenomenologically by the fitting procedure. For instance, the parametrizations SLy (Chabanat et al. 1997) have been specifically constructed for neutron star studies by fitting a 'realistic' equation of state of neutron matter up to very high densities $\sim 10\rho_0$. Besides, it is worth mentioning that soon after such effective forces were introduced, Cameron (1959) applied them to neutron stars and showed that the maximum mass $\sim 2\,{\rm M}_\odot$ is compatible with the scenario of neutron star formation from supernova explosions. The main limitation of these effective forces is that they describe only nucleonic degrees of freedom. At densities above $\sim 3\rho_0$, other particles like hyperons are likely to appear (Haensel et al. 2006). Nevertheless, let us remark that for the most precisely measured neutron star masses in binary radio pulsars, their central densities lie below ~ 3–$4\rho_0$ depending on the equation of state [see e.g. chapter 6 from Haensel et al. (2006) and in particular their fig. 6.3]. Our main motivation for using such kind of effective Hamiltonian is the perspective of a unified treatment of the interior of neutron stars, including not only the liquid core but also the solid crust whose microscopic description starting from the bare nucleon–nucleon interaction is not feasible.

Assuming that the matter in neutron star cores is not polarized for the densities of interest as suggested by many-body calculations (see e.g. Bombaci et al. 2006), the nucleon energy density associated with the force (97) can be calculated using the method outlined in the classic paper of Vautherin & Brink (1972) and is given by an

expression of the form

$$U_{\rm N}\left\{n_{\rm n},n_p\right\} = n_{\rm b}mc^2 + \frac{\hbar^2}{2m}\tau_{\rm b} + B_1 n_{\rm b}^2 + B_2(n_{\rm n}^2+n_p^2) + B_3 n_{\rm b}\tau_{\rm b} + B_4(n_{\rm n}\tau_{\rm n}+n_p\tau_p) + B_5 n_{\rm b}^{2+\alpha} + B_6 n_{\rm b}^{\alpha}(n_{\rm n}^2+n_p^2), \tag{99}$$

where

$$\tau_{\rm n} = \frac{3}{5}(3\pi^2)^{2/3}n_{\rm n}^{5/3}, \quad \tau_p = \frac{3}{5}(3\pi^2)^{2/3}n_p^{5/3}, \tag{100}$$

are, respectively, the neutron and proton kinetic energy densities (in units of $\hbar^2/2m$), and $\tau_{\rm b} = \tau_{\rm n} + \tau_p$. The B-coefficients are related to the parameters of the force by the following expressions:

$$B_1 = \frac{t_0}{2}\left(1+\frac{x_0}{2}\right) \tag{101}$$

$$B_2 = -\frac{t_0}{2}\left(x_0+\frac{1}{2}\right) \tag{102}$$

$$B_3 = \frac{1}{4}\left[t_1\left(1+\frac{x_1}{2}\right)+t_2\left(1+\frac{x_2}{2}\right)\right] \tag{103}$$

$$B_4 = -\frac{1}{4}\left[t_1\left(x_1+\frac{1}{2}\right)-t_2\left(x_2+\frac{1}{2}\right)\right] \tag{104}$$

$$B_5 = \frac{t_3}{12}\left(1+\frac{x_3}{2}\right) \tag{105}$$

$$B_6 = -\frac{t_3}{12}\left(x_3+\frac{1}{2}\right). \tag{106}$$

Analytic expressions of the effective masses $m_\star^n$ and $m_\star^p$ for the force (97) have been recently obtained by Chamel & Haensel (2006). Introducing the parameter $\beta_3 = 2mB_3/\hbar^2$, the coefficients of the mobility matrix, given by equations (56) and (57), can be expressed as

$$\mathcal{K}^{nn} = \frac{m}{n_{\rm n}}\frac{1+\beta_3 n_{\rm n}}{1+\beta_3 n_{\rm b}} \tag{107}$$

$$\mathcal{K}^{pp} = \frac{m}{n_p}\frac{1+\beta_3 n_p}{1+\beta_3 n_{\rm b}} \tag{108}$$

$$\mathcal{K}^{np} = \mathcal{K}^{pn} = m\frac{\beta_3}{1+\beta_3 n_{\rm b}}. \tag{109}$$

Note that as a consequence of the isospin symmetry of the nucleon–nucleon interactions, we have $\mathcal{K}^{nn}\{n_{\rm n},n_p\} = \mathcal{K}^{pp}\{n_p,n_{\rm n}\}$ and $\mathcal{K}^{np}$ (therefore λ_1) does not depend on the matter composition but only on the *total* baryon density $n_{\rm b} = n_{\rm n} + n_p$. This means that entrainment effects are not affected by the various chemical reactions that may occur inside the core, as discussed in Section 7. In the high-density limit $\beta_3 n_{\rm n} \gg 1$ and $\beta_3 n_p \gg 1$, all the elements of the mobility matrix become equal to $\mathcal{K}^{qq'} \to m/n_{\rm b}$. As a consequence, the non-relativistic effective masses tend to $m_\star^q/m \to {\rm n_q/n_b}$. This asymptotic limit which corresponds to the strongest entrainment effects (see the discussion of Section 3) is never reached in neutron star core for the nucleon–nucleon interactions considered in this work, since m/β_3 is typically of the order of $\sim 10\rho_0$ (see Table 3).

9 CHOICE OF EFFECTIVE MICROSCOPIC HAMILTONIAN

We have selected effective forces according to the following criteria. First of all, the chosen forces have to yield reasonable values of the 'semi-empirical' saturation properties of infinite uniform symmetric nuclear matter, namely the equilibrium or saturation density n_0 (or the mass density $\rho_0 = n_0 m$), the binding energy per nucleon

$$a_v = \frac{U_{\rm N}\{n_0/2,n_0/2\}}{n_0} - mc^2, \tag{110}$$

the symmetry energy coefficient

$$a_{\rm s} = \frac{1}{2}\frac{\partial^2}{\partial I^2}\left(\frac{U_{\rm N}}{n_{\rm b}}\right)\bigg|_{I=0,n_{\rm b}=n_0} \tag{111}$$

with $I = (n_{\rm n}-n_p)/n_{\rm b}$ and the incompressibility modulus

$$K_\infty = 9n_0^2\frac{\partial^2}{\partial n_{\rm b}^2}\left(\frac{U_{\rm N}\{n_{\rm b}/2,n_{\rm b}/2\}}{n_{\rm b}}\right)\bigg|_{\rm n_b=n_0}. \tag{112}$$

Global fits to essentially all the available experimental nuclear mass data yield $n_0 \simeq 0.16\,{\rm fm}^{-3}$, $a_v \simeq -16$ MeV, $a_{\rm s} \simeq 28$–35 MeV and $K_\infty \simeq 220$–240 MeV (Lunney, Pearson & Thibault 2003). Due to the strong interactions, the mass of the individual nucleons in nuclear matter is different from the bare mass and can be written as

$$\frac{m}{m_{\rm n}^*} = (1+I)\frac{m}{m_{\rm s}^*} - I\frac{m}{m_v^*}, \quad \frac{m}{m_p^*} = (1-I)\frac{m}{m_{\rm s}^*} + I\frac{m}{m_v^*} \tag{113}$$

in which $m_{\rm s}^*$ and m_v^* are the so-called isoscalar and isovector effective masses, respectively (see e.g. Farine, Pearson & Tondeur 2001). The isovector effective mass is a crucial microscopic input since it directly controls the strength of entrainment effects in neutron–proton mixtures. Indeed, the parameter β_3 which determines the mobility matrix, equations (107), (108) and (109), is given by

$$n_{\rm b}\beta_3 = \frac{m}{m_v^*} - 1. \tag{114}$$

In principle, this isovector effective mass can be determined from measurements of the giant isovector electric dipole resonance in finite nuclei (consisting of relative motions between neutrons and protons). Nevertheless, estimates are model dependent providing values $m_v^*/m \sim 0.7$–1 at saturation density (see in particular the discussion of Lunney et al. 2003 in section III-B-5-e). Microscopic many-body calculations in infinite uniform nuclear matter starting from the bare nucleon–nucleon interaction lead to an isovector effective mass around $m_v^*/m \sim 0.7$ (see e.g. Zuo et al. 2006). Besides, we consider only those effective forces that have been constrained to fit the uniform infinite neutron matter equation of state. Otherwise, these effective forces could not be reliably extrapolated to the neutron-rich matter inside neutron star core.

The main deficiencies of effective forces are the existence of instabilities that are not found by microscopic calculations (Margueron, Navarro & van Giai 2002; Agrawal, Shlomo & Au 2004; Lesinski et al. 2006). Especially, many Skyrme forces predict a spurious ferromagnetic transition in neutron matter above some critical densities. We thus require that no such instabilities occur in the density range of interest $\rho < 3\rho_0$ by imposing that the dimensionless Landau parameter, usually noted as G_0, be greater than -1 in neutron matter (following the analysis of Margueron et al. 2002). It turns out that this criterion is very restrictive. Several forces that reproduce reasonably well both the saturation properties of symmetric nuclear matter and the neutron matter equation of state do not pass this test. For instance, the parametrization RATP (Rayet et al. 1982), which was the first attempt to construct an effective force

for astrophysical applications, predicts that neutron matter becomes spin polarized slightly above saturation density $\simeq 0.175$ fm^{-3} (the density for the onset of instability is obtained by solving $G_0 = -1$). Likewise, the forces SkM and Skyrme 1′, which have been applied to study dense matter in neutron stars and supernova cores (Bonche & Vautherin 1982; Lattimer et al. 1985; Lassaut et al. 1987; Lorenz, Ravenhall & Pethick 1993), yield a ferromagnetic transition density in neutron matter $\simeq 0.212$ and $\simeq 0.256$ fm^{-3}, respectively. We have found that only the forces of the Saclay–Lyon group (Chabanat et al. 1997, 1998a,b) and the recent parametrization LNS (Cao et al. 2006) satisfy all the above conditions. They predict a ferromagnetic instability in neutron matter like the other forces, but at significantly higher densities $\sim$3–4ρ_0 which we do not consider in this work. The force LNS seems the most appropriate to describe neutron star core since it was constructed so as to reproduce recent results of microscopic diagrammatic calculations (based on Brueckner theory) of infinite uniform nuclear matter with two- as well as three-body forces. In particular, this effective force not only fits well the energy per nucleon in symmetric and asymmetric nuclear matter, but also fits the nucleon effective masses for different asymmetries and different densities which directly determine the entrainment coefficients as previously discussed. Nevertheless, the SLy forces, which were constrained to reproduce some properties of finite nuclei (apart from the other constraints that we imposed), would be preferable if not only the liquid core but also the crust layers would have to be described with the same underlying microscopic Hamiltonian. Besides, the equation of state of neutron star matter with the force SLy4 has been tabulated and widely applied (Haensel & Potekhin 2004). For comparison, we have also considered the parametrization NRAPR (Steiner et al. 2005) since it was adjusted on the realistic equation of state of Akmal et al. (1998). Nevertheless, this force leads to a ferromagnetic instability at rather low density $\rho \lesssim 2\rho_0$.

The parameters of the forces and the associated B-coefficients introduced in Section 8 are given in Tables 1 and 2, respectively. The nuclear matter properties predicted by these forces are summarized in Table 3. Fig. 1 shows the binding energy per particle in uniform infinite neutron matter defined by $E/A = U_{\rm N}\{n_{\rm n}, 0\}/n_{\rm n} - mc^2$. Let us stress that the LNS force was fitted to the latest results of many-body calculations with two- and three-body forces, while the forces of the Lyon group were adjusted to reproduce an older neutron matter equation of state based on variational methods.

Figs 2–4 show the equilibrium composition of cold neutron star matter, composed of neutrons, protons, electrons and muons, obtained by solving equations (80), (88) and (89). The figures show the electron, muon and proton fractions, defined, respectively, by $n_e/n_{\rm b}, n_\mu/n_{\rm b}$ and $n_p/n_{\rm b}$, as a function of the mass-energy density $\rho = U_{\rm ins}/c^2$, which is approximately given by $\rho \simeq n_{\rm b} m$ for $n_{\rm b} <$

Table 1. Parameters of the chosen Skyrme forces. The units of energy and length are MeV and fm, respectively.

	SLy4	LNS	NRAPR
t_0	−2488.91	−2484.97	−2719.7
t_1	486.82	266.735	417.64
t_2	−546.39	−337.135	−66.687
t_3	13777.0	14588.2	15042.0
α	1/6	1/6	0.14416
x_0	0.834	0.06277	0.16154
x_1	−0.344	0.65845	−0.0047986
x_2	−1	−0.95382	0.027170
x_3	1.354	−0.03413	0.13611

Table 2. B-coefficients of the chosen Skyrme forces. The units of energy and length are MeV and fm, respectively.

	B_1	B_2	B_3	B_4	B_5	B_6
SLy4	−1763.39	1660.1	32.473	49.3128	1925.34	−2128.55
LNS	−1281.48	699.233	44.5497	−39.0001	1194.94	−566.35
NRAPR	−1469.69	899.595	85.0067	−55.9836	1338.81	−797.364

Table 3. Properties of infinite uniform symmetric nuclear matter for the chosen Skyrme forces. n_0 (fm^{-3}) is the nuclear saturation density, a_v (MeV) is the binding energy per nucleon of infinite symmetric nuclear matter, $a_{\rm s}$ (MeV) is the symmetry energy coefficient, K_∞ (MeV) is the compression modulus, $m_{\rm s}^*/m$ and m_v^*/m are the isoscalar and isovector effective masses, respectively, $n_{\rm f}$ (fm^{-3}) is the density at which a ferromagnetic instability occurs in neutron matter. Realistic values of these parameters are $n_0 \simeq 0.16$ fm^{-3}, $a_v \simeq -16$ MeV, $a_{\rm s} \simeq$ 28–35 MeV, $K_\infty \simeq$ 220–240 MeV, $m_{\rm s}^*/m \sim$ 0.6–0.9, $m_v^*/m \sim$ 0.7–1 (Lunney et al. 2003).

	n_0	a_v	$a_{\rm s}$	K_∞	$m_{\rm s}^*/m$	m_v^*/m	$n_{\rm f}$
SLy4	0.160	−15.97	32.0	229.9	0.696	0.801	0.59
LNS	0.175	−15.32	33.4	210.9	0.827	0.728	0.62
NRAPR	0.1606	−15.86	32.79	225.7	0.695	0.605	0.28

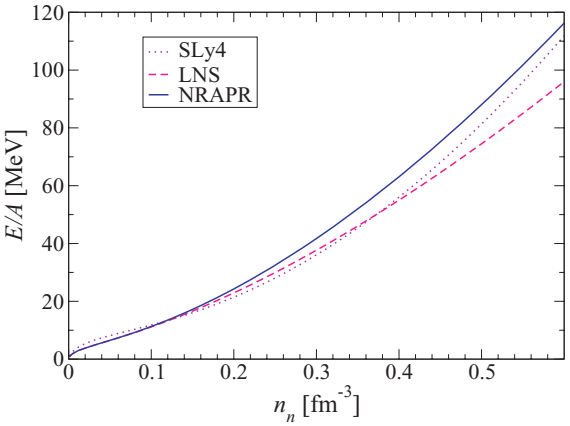

Figure 1. Binding energy per particle of uniform infinite neutron matter for the SLy4, LNS and NRAPR effective forces.

$3n_0$. All forces predict the appearance of muons at $n_{\rm b} \simeq 0.12$ fm^{-3} or $\rho \simeq 2 \times 10^{14}$ g cm^{-3}. The forces LNS and NRAPR yield similar composition. They both predict a slightly larger (respectively smaller) proton fraction than the force SLy4 above (respectively below)ρ_0. This can be understood by remarking that equation (88) can be approximately written as (Muther, Prakash & Ainsworth 1987)

$$\hbar c (3\pi^2 n_{\rm b} x_e)^{1/3} \approx 4\mathcal{S}\{n_{\rm b}\}(1 - 2x_p), \tag{115}$$

where the symmetry energy $\mathcal{S}\{n_{\rm b}\}$ defined by

$$\mathcal{S}\{n_{\rm b}\} = \frac{U_{\rm N}\{n_{\rm b}, 0\}}{n_{\rm b}} - \frac{U_{\rm N}\{n_{\rm b}/2, n_{\rm b}/2\}}{n_{\rm b}} > 0 \tag{116}$$

represents the cost in (nuclear) energy per particle to replace protons by neutrons in symmetric nuclear matter. From equation (115), we have

$$x_p \approx x_e \approx \left(\frac{4\mathcal{S}\{n_{\rm b}\}}{\hbar c}\right)^3 \frac{1}{3\pi^2 n_{\rm b}}. \tag{117}$$

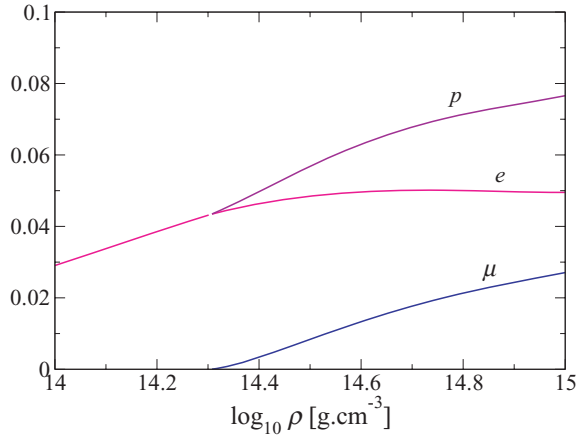

Figure 2. Equilibrium fractions $n_{\rm x}/n_{\rm b}$ of protons (p), electrons (e) and muons (μ) inside neutron star core predicted by the SLy4 effective force.

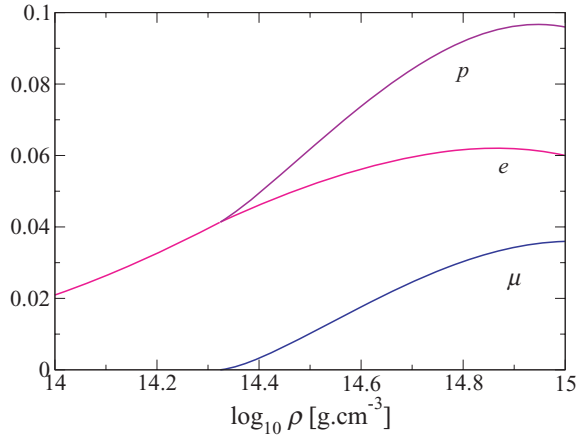

Figure 3. Equilibrium fractions $n_{\rm x}/n_{\rm b}$ of protons (p), electrons (e) and muons (μ) inside neutron star core predicted by the LNS effective force.

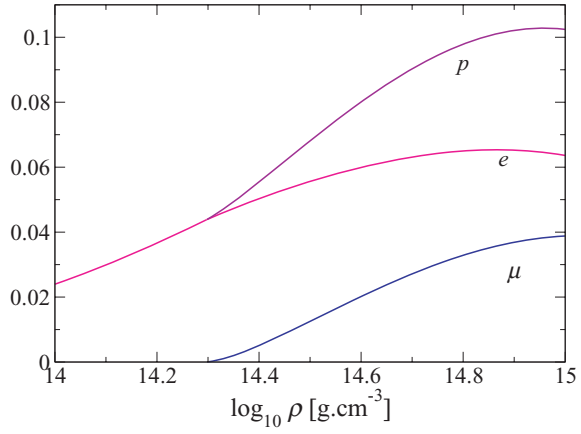

Figure 4. Equilibrium fractions $n_{\rm x}/n_{\rm b}$ of protons (p), electrons (e) and muons (μ) inside neutron star core predicted by the NRAPR effective force.

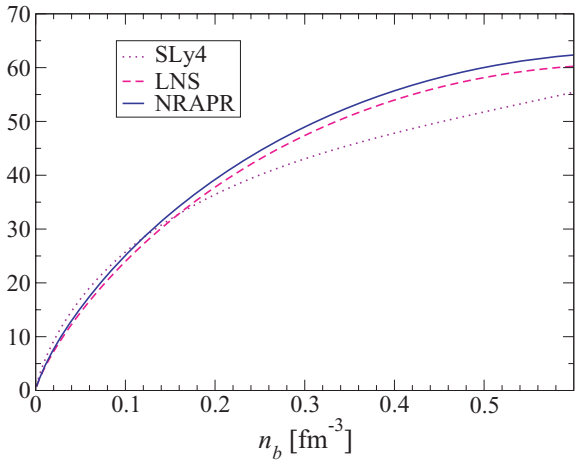

Figure 5. Symmetry energy $\mathcal{S}\{n_{\rm b}\}$ (in MeV) for the SLy4, LNS and NRAPR effective forces as a function of the baryon density $n_{\rm b} = n_{\rm n} + n_p$.

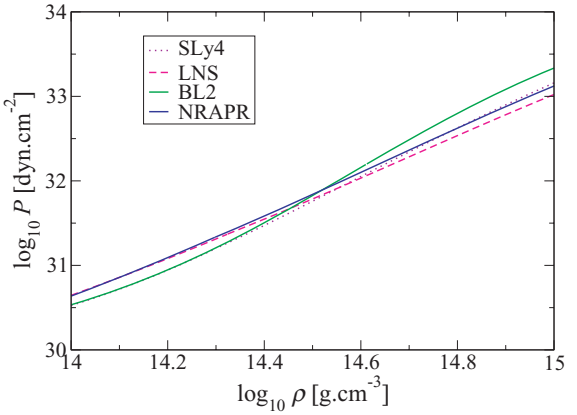

Figure 6. Static pressure of neutron star matter in equilibrium for the Skyrme effective forces and for the BL2 relativistic mean field model.

As can be seen in Fig. 5, the forces LNS and NRAPR yield a larger (respectively smaller) symmetry energy than the force SLy4 above (respectively below) the saturation density n_0 (note that the symmetry energy coefficient $a_{\rm s} \simeq \mathcal{S}\{n_0\}$).

Fig. 6 shows the static pressure (90) of $npe\mu$ matter in equilibrium as a function of the mass-energy density $\rho = U_{\rm ins}/c^2$. In Figs 7–9, we compare the effective masses defined by equation (56) for the two Skyrme forces. In both cases, the neutron effective mass is close to the bare nucleon mass while the proton effective mass is significantly reduced. This is consistent with the inequality (58) which implies that

$$\frac{m^n_\star}{m} - \frac{m^p_\star}{m} > I, \tag{118}$$

with $I = (n_{\rm n} - n_p)/n_{\rm b}$. The relativistic effective masses defined by equation (61) are shown in Figs 10–12. For simplicity, we have considered that neutrons and protons are comoving so that the effective masses are given by

$$\frac{\widetilde{m}^q_\star}{m} = \frac{m^q_\star}{m} + \frac{\mu_q}{mc^2} - 1. \tag{119}$$

These relativistic effective masses are significantly different compared to the non-relativistic ones. In particular, both nuclear forces predict that the neutron relativistic effective mass is larger than the

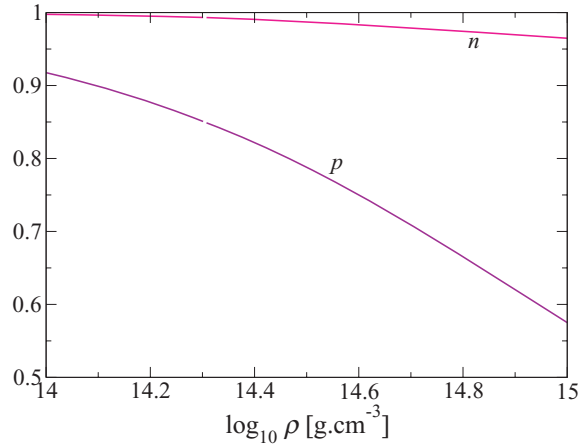

Figure 7. Neutron and proton effective masses, respectively, $m^n_\star/m$ and $m^p_\star/m$, defined by equation (56), in neutron star matter in equilibrium for the SLy4 effective force.

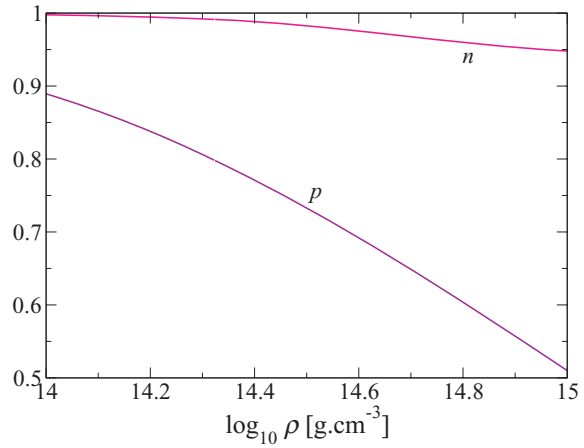

Figure 8. Neutron and proton effective masses, respectively $m^n_\star/m$ and $m^p_\star/m$, defined by equation (56), in neutron star matter in equilibrium for the LNS effective force.

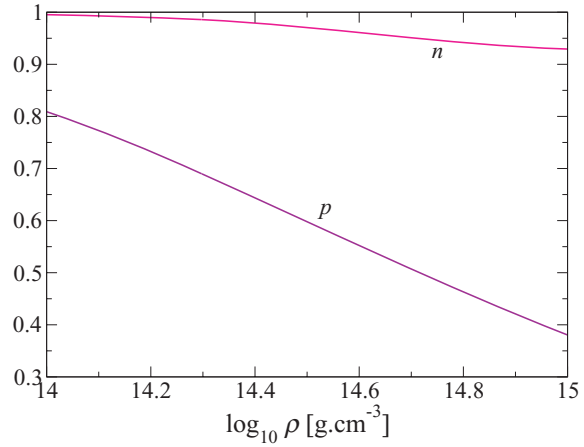

Figure 9. Neutron and proton effective masses, respectively $m^n_\star/m$ and $m^p_\star/m$, defined by equation (56), in neutron star matter in equilibrium for the NRAPR effective force.

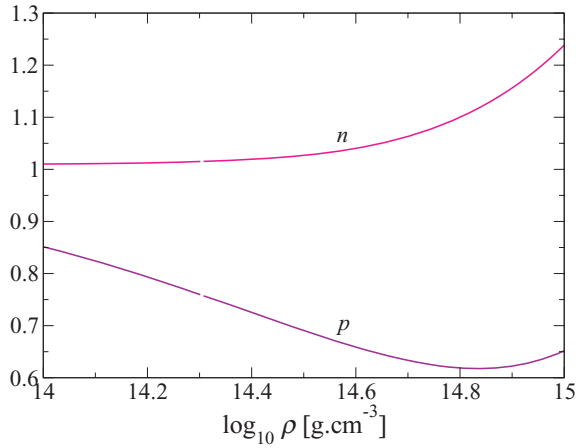

Figure 10. Relativistic neutron and proton effective masses, respectively $\widetilde{m}^n_\star/m$ and $\widetilde{m}^p_\star/m$, defined by equation (61), in neutron star matter in equilibrium for the SLy4 effective force. Neutrons and protons are comoving.

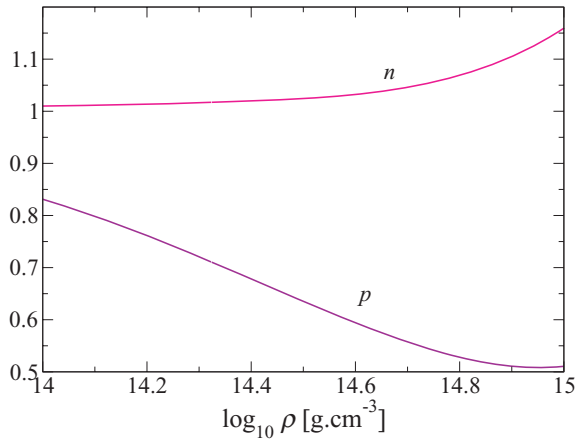

Figure 11. Relativistic neutron and proton effective masses, respectively $\widetilde{m}^n_\star/m$ and $\widetilde{m}^p_\star/m$, defined by equation (61), in neutron star matter in equilibrium for the LNS effective force. Neutrons and protons are comoving.

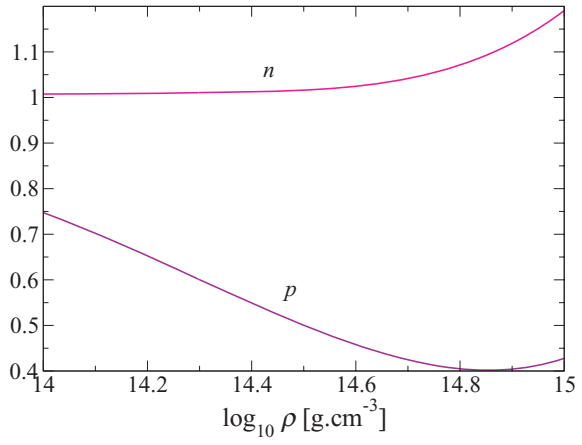

Figure 12. Relativistic neutron and proton effective masses, respectively $\widetilde{m}^n_\star/m$ and $\widetilde{m}^p_\star/m$, defined by equation (61), in neutron star matter in equilibrium for the NRAPR effective force. Neutrons and protons are comoving.

bare mass. Moreover, from equations (118) and (88), we have

$$\frac{\widetilde{m}^n_\star}{m} - \frac{\widetilde{m}^p_\star}{m} = \frac{m^n_\star}{m} - \frac{m^p_\star}{m} + \frac{\mu_e}{mc^2} > I + \frac{\mu_e}{mc^2}, \tag{120}$$

so that the splitting of the relativistic effective masses is larger than that of the non-relativistic ones since $\mu_e \geq 0$.

10 COMPARISON WITH RELATIVISTIC MEAN FIELD MODELS

A few years ago, Comer & Joynt (2003) developed relativistic two-fluid models of superfluid neutron star cores. They have determined the master function Λ using the effective relativistic mean field theory (Glendenning 2000). In the model they considered, the interactions between nucleons arise from the exchange of two massive mesons: the scalar meson σ with mass m_σ and the vector meson ω_μ with mass m_ω. The former accounts for the long-range attractive part of the nucleon–nucleon interaction while the latter gives rise to the short-range repulsive part. In the nuclear field theory, particles are described by a microscopic Lagrangian density $\mathcal{L}$ (not to be confused with the macroscopic Lagrangian density Λ of the fluids) given by (using units $c = \hbar = 1$)

$$\begin{aligned}\mathcal{L} = {} & \bar{\psi}[\gamma^\mu \mathrm{i} D_\mu - m_\mathrm{D}]\psi + \frac{1}{2}\left[(\partial^\mu\sigma)(\partial_\mu\sigma) - m_\sigma^2\sigma^2\right] \\ & - \frac{1}{4}\omega^{\mu\nu}\omega_{\mu\nu} + \frac{1}{2}m_\omega^2\omega_\mu\omega^\mu\end{aligned} \tag{121}$$

with the nucleon field ψ and the antisymmetric tensor $\omega_{\mu\nu} \equiv \partial_\mu\omega_\nu - \partial_\nu\omega_\mu$ (γ^μ denote the Dirac matrices and $\bar{\psi} \equiv \psi^\dagger\gamma^0$). The nucleon–meson couplings are introduced in the gauge covariant derivative

$$D_\mu = \partial_\mu + \mathrm{i}\, g_\omega \omega_\mu \tag{122}$$

and in the Dirac effective nucleon mass

$$m_\mathrm{D} = m - g_\sigma\sigma \tag{123}$$

where g_ω and g_σ are dimensionless coupling constants. The field equations, which actually only depend on the quantities $c_\sigma^2 = g_\sigma^2/m_\sigma^2$ and $c_\omega^2 = g_\omega^2/m_\omega^2$ in uniform infinite matter, are solved in the Hartree approximation (exchange terms are neglected) ignoring the contributions of antiparticles (the so-called no Dirac sea approximation).

As for the non-relativistic energy density functional theory discussed in Section 9, the free parameters of the model have to be determined by fitting to some nuclear matter properties. Comer & Joynt (2003) adopted two parameter sets from Glendenning (2000) (chapter 4, table 4.4). However, these parameters were not obtained for the Lagrangian density given by equation (121) but for a more elaborate class of models which includes scalar self-interactions as well as the vector–isovector rho meson. As a result, by dropping these extra terms in the Lagrangian density $\mathcal{L}$, the resulting $\sigma - \omega$ models considered by Comer & Joynt (2003) predict unphysical nuclear matter properties, as can be seen in Table 5 (see the discussion in Section 9). Besides, these models predict that neutron matter is bound as shown in Fig. 14, unlike quantum many-body calculations using realistic nucleon–nucleon interactions. Note also that these models predict that neutrons and protons have the same (Dirac) effective mass m_D for any nuclear asymmetry $I = (n_\mathrm{n} - n_p)/n_\mathrm{b}$, in contradiction to microscopic calculations (see e.g. van Dalen & Fuchs 2007, especially their figure 4). As such, these models are therefore unsuitable for applications to neutron stars as pointed out by Glendenning (2000). In order to reproduce the properties of finite nuclei and infinite nuclear matter with the same level of accuracy as the non-relativistic effective forces discussed in Section 9, other mesons must be included. Besides, non-linear self-meson interactions must be introduced (see e.g. chapter 4 of Glendenning 2000).

Table 4. Parameters of the $\sigma - \omega$ relativistic mean field models discussed in this work. GLI and GLII are the models proposed by Glendenning (2000) and employed by Comer & Joynt (2003) after dropping scalar self-interactions and the rho meson. The models BL1–BL4 are new parameter sets introduced in this work (the coupling constants are given in fm^2). Note that for the baryon mass we have taken the average of the neutron and proton masses as Comer & Joynt (2003).

	c_σ^2	c_ω^2
GLI	12.684	7.148
GLII	8.403	4.233
BL1	14.6063	11.0544
BL2	9.3353	7.2624
BL3	23.2707	14.4061
BL4	7.79346	6.06748

For the present time, we will restrict the discussion of the entrainment effects to the $\sigma - \omega$ model. The models considered by Comer & Joynt (2003) can be significantly improved (keeping in mind the inherent limitations of such models) by simply refitting the parameters. With only two free parameters c_σ and c_ω, only two of the symmetric infinite nuclear matter properties listed in Table 3 can be fitted exactly. We have constructed three new parameter sets BL1–BL3 by fixing the saturation density to $n_0 = 0.16$ fm^{-3} and (i) the binding energy per nucleon to $a_v = -16$ MeV for BL1, (ii) the Dirac effective mass to $m_\mathrm{D} = 0.7\, m$ for BL2 and (iii) the symmetry energy to $a_\mathrm{s} = 28$ MeV for BL3 (the fitting procedure did not converge for $a_\mathrm{s} = 30$ MeV). The parameters of these new models are given in Table 4. As can be seen in comparing Table 3 and 5, the overall agreement with empirical nuclear data is still very poor reflecting the lack of flexibility of these $\sigma - \omega$ models. The most important constraint for application to neutron stars is to reproduce at least the equation of state of neutron matter. We have thus constructed the parameter set BL4 by fitting the realistic equation of state of Akmal et al. (1998). The result of the fit is shown in Fig. 14, as well as the predictions of the other mean field models. This should be compared with the results of non-relativistic effective forces in Fig. 1. Note that the parameter sets GLI, GLII and BL3 incorrectly predict the existence of bound neutron matter. From these four models, it seems that the best compromise is achieved for the parameter set BL2, yielding reasonable values of the saturation density, compression modulus, Dirac effective mass (which is an important quantity for entrainment effects as discussed in Section 9) together with a fairly good fit of the neutron matter equation of state. Note, however, that this model is still very crude compared to the SLy4 or LNS Skyrme forces presented in Section 9. In particular, the values of the symmetry energy a_s and the binding energy per nucleon a_v, which are two basic nuclear matter properties, are unrealistic.

We have applied the general expressions derived by Comer & Joynt (2003) within the $\sigma - \omega$ mean field models to evaluate the entrainment parameters and to compare the results with those obtained using the non-relativistic effective energy density functional theory. We have greatly improved the models considered by Comer & Joynt (2003) (i) by refitting the meson coupling constants leading to a better agreement with nuclear data as discussed previously and

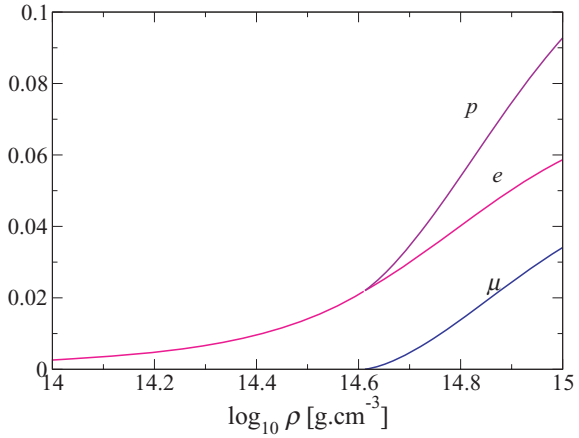

Figure 13. Equilibrium fractions $n_{\rm x}/n_{\rm b}$ of protons (p), electrons (e) and muons (μ) inside neutron star core predicted by the BL2 relativistic mean field model.

(ii) by including muons which affect the composition of neutron star core and contribute to the pressure. Leptons are treated as ideal relativistic Fermi gases as discussed in Section 9. The parameters λ_0 and λ_1 in the expansion of the master function Λ, introduced in Section 4, are given by

$$\lambda_0 = \Lambda|_0 - U_{\rm L}\left\{n_\mu\right\}, \qquad \lambda_1 = -\mathcal{A}|_0 \tag{124}$$

where $\mathcal{A}|_0$ and $\Lambda|_0$ are given by equations (63) and (A8), respectively, in Comer & Joynt (2003). Note that we have added the muon contribution in the Lagrangian density. Using the nucleon chemical potentials given by equations (A9) and (A10) of that paper, together with the lepton chemical potentials defined by equation (23), we have determined the equilibrium composition of the neutron star core assuming comoving particles as discussed in Section 7. Results are shown in Fig. 13 for the parameter set BL2. The proton fraction is very small at low densities unlike that predicted by non-relativistic effective forces. As discussed in Section 9, this can be understood from the very small (incorrect) value of the symmetry energy $a_{\rm s}$ at saturation density (see Table 5). As can be seen in Fig. 6, the equation of state is, however, similar to that obtained for the non-relativistic effective nucleon–nucleon interactions. The reason is that matter in neutron star core is almost pure neutron matter and all models SLy4, LNS and BL2 reproduce reasonably well the neutron matter equation of state (see Figs 1 and 14).

Table 5. Properties of infinite uniform symmetric nuclear matter for $\sigma-\omega$ relativistic mean field models. The quantities shown are the same as those introduced in Table 3. Realistic values are $n_0 \simeq 0.16$ fm^{-3}, $a_v \simeq -16$ MeV, $a_{\rm s} \simeq 28$–35 MeV, $K_\infty \simeq 220$–240 MeV (Lunney et al. 2003). Note that recent relativistic many-body calculations by van Dalen & Fuchs (2007) predict that the Dirac effective mass at saturation is $m_{\rm D} \simeq 0.7\,m$. GLI and GLII are the models employed by Comer & Joynt (2003) while models BL1–BL4 are new parameter sets introduced in this work.

	n_0	a_v	$a_{\rm s}$	K_∞	$m_{\rm D}/m$
GLI	0.28	−66.43	34.69	2117.5	0.385
GLII	0.41	−66.69	41.29	2252.0	0.407
BL1	0.16	−16	20.09	674.0	0.543
BL2	0.16	−1.70	16.29	249.0	0.700
BL3	0.16	−72.24	28	2217.4	0.338
BL4	0.14	1.7358	13.88	130.5	0.774

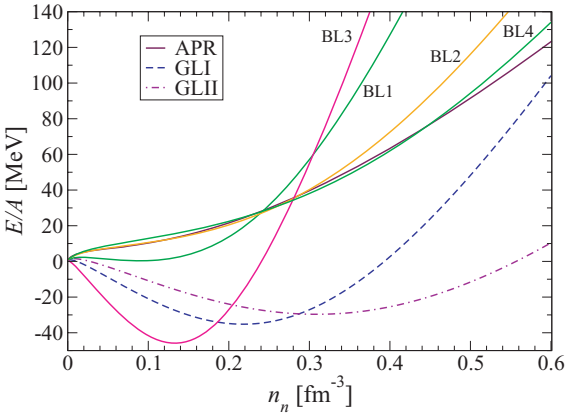

Figure 14. Energy per particle of uniform infinite neutron matter for relativistic $\sigma-\omega$ mean field models. The curve labelled APR is the 'realistic' equation of state of Akmal et al. (1998), using the analytical fit of Heiselberg & Hjorth-Jensen (2000). The rest-mass energy has been subtracted out. GLI and GLII are the models used by Comer & Joynt (2003). BL1–BL4 are the parameter set constructed in this work.

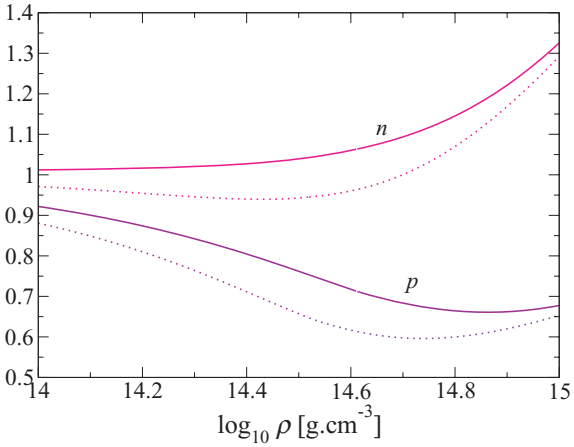

Figure 15. Relativistic neutron and proton effective masses, respectively $\widetilde{m}^n_\star/m$ and $\widetilde{m}^p_\star/m$, defined by equation (61), in neutron star matter in equilibrium for the BL2 (solid lines) and GLI (dotted lines) relativistic mean field models. Neutrons and protons are comoving.

The relativistic effective masses introduced in Section 4 are given by

$$\widetilde{m}^n_\star = n_{\rm n}\,\mathcal{B}|_0, \qquad \widetilde{m}^p_\star = n_p\,\mathcal{C}|_0, \tag{125}$$

where $\mathcal{B}|_0$ and $\mathcal{C}|_0$ are given by equations (64) and (65), respectively, in Comer & Joynt (2003). As shown in Fig. 15, the neutron effective mass predicted by the model GL2 is larger than the bare nucleon mass while the proton effective mass is smaller, as obtained for non-relativistic models. For comparison, we have also plotted the effective masses obtained with the model GLI considered by Comer & Joynt (2003). The neutron effective mass obtained with this parameter set is decreased at low densities compared to the ordinary mass in contradiction to previous results. This is a consequence of the fact that the model GLI predicts (incorrectly) that neutron matter is bound, as shown in Fig. 14, so that $\mu_{\rm n} < mc^2$.

11 CONCLUSION

The recent detection of QPOs in SGR (most likely associated with seismic vibrations triggered by magnetic crust quakes) and future observations with gravitational wave detectors offer new possibilities to probe the interior of neutron stars and to test the theories of dense matter. Nevertheless, the reliable identification of the various oscillation modes calls for a consistent theoretical description of the star. As a first step towards this goal, we have constructed fully self-consistent relativistic two-fluid models of neutron star cores, composed of superfluid neutrons and a conglomerate of protons, electrons and possibly muons. The mutual entrainment effects between the two fluids, resulting from the strong nucleon–nucleon interactions, are properly taken into account. We have determined the expression of the Lagrangian density in the variational framework developed by Brandon Carter and co-workers. We have also shown how to make the correspondence with non-relativistic models by applying the 4D covariant formulation of Newtonian hydrodynamics of Carter & Chamel (2004). We have determined all the coefficients of these models consistently with the *same* microscopic approach. In the perspective of describing not only the liquid core of neutron stars but also the crust layers, we have employed the nuclear energy density functional theory which has been already successfully applied to study both isolated nuclei and infinite nuclear matter. As an example, we have calculated the composition, the equation of state and the entrainment matrix of neutron star core for three different nuclear models: the popular SLy4 model for which the equation of state of both the crust and the liquid core has already been tabulated (Haensel & Potekhin 2004) and the more recent LNS and NRAPR models which have been entirely constructed from recent realistic many-body calculations. For comparison, we have also considered relativistic $\sigma - \omega$ mean field models that have been first applied by Comer & Joynt (2003). We have improved their models by refitting the parameters in order to obtain a better agreement with nuclear data, but still we could not reach the same level of accuracy as the non-relativistic models mentioned above. This would require the introduction of additional meson fields, especially the rho meson. Besides, self-meson couplings should be taken into account. Numerical calculations with both effective energy density functional and relativistic mean field models have shown that the dynamical effective nucleon masses arising from entrainment effects are smaller than the ordinary mass in the Newtonian case. Relativistic effects increase effective masses, since all forms of internal energy contribute to the mass. A rather unexpected consequence, which has not been usually discussed in the literature, is that relativistic effective masses can be even larger than the bare mass in the liquid core of neutron stars.

ACKNOWLEDGMENTS

This work was financially supported by FNRS (Belgium). The author is grateful to Brandon Carter for valuable comments during the completion of this work.

REFERENCES

Agrawal B. K., Shlomo S., Au V. K., 2004, Phys. Rev. C, 70, 057302
Akmal A., Pandharipande V. R., Ravenhall D. G., 1998, Phys. Rev. C, 58, 1804
Andersson N., Comer G. L., 2001, MNRAS, 328, 1129
Andersson N., Comer G. L., 2007, Living Rev. Relativ., 10
Anderson P. W., Itoh N., 1975, Nat, 256, 25
Andersson N., Kokkotas K. D., 2005, in Tamvakis K., ed., Lecture Notes in Phys. Vol. 653, The Physics of the Early Universe. Springer-Verlag, Berlin, p. 255
Andersson N., Comer G. L., Langlois D., 2002, Phys. Rev. D, 66, 104002
Barat C. et al., 1983, A&A, 126, 400
Baym G., Pethick C. J., Pines D., 1969, Nat, 224, 673
Bender M., Heenen P. H., Reinhard P. G., 2003, Rev. Modern Phys., 75, 121
Bombaci I., Polls A., Ramos A., Rios A., Vidaña I., 2006, Phys. Lett. B, 632, 638
Bonche P., Vautherin D., 1982, A&A, 112, 268
Cameron A. G., 1959, ApJ, 130, 884
Cao L. G., Lombardo U., Shen C. W., Giai N. V., 2006, Phys. Rev. C, 73, 014313
Carter B., 1989, in Anile A., Choquet-Bruhat Y., eds, Relativistic Fluid Dynamics. Springer-Verlag, Berlin, p. 1
Carter B., 2000, in Bunkov Y. M., Godfrin H., eds, NATO Advanced Study Inst. Ser. Vol. C549, Topological Defects and Non-equilibrium Dynamics of Phase Transitions. Kluwer Academic Publisher, Dordrecht, p. 267
Carter B., Chamel N., 2004, Int. J. Mod. Phys. D, 13, 291
Carter B., Chamel N., 2005a, Int. J. Mod. Phys. D, 14, 717
Carter B., Chamel N., 2005b, Int. J. Mod. Phys. D, 14, 749
Carter B., Chamel N., Haensel P., 2005, Nucl. Phys. A, 748, 675
Carter B., Chachoua E., Chamel N., 2006a, Gen. Relativ. Gravit., 38, 83
Carter B., Chamel N., Haensel P., 2006b, Int. J. Mod. Phys. D, 15, 777
Chabanat E., Bonche P., Haensel P., Meyer J., Schaeffer R., 1997, Nucl. Phys. A, 627, 710
Chabanat E., Bonche P., Haensel P., Meyer J., Schaeffer R., 1998a, Nucl. Phys. A, 643, 441
Chabanat E., Bonche P., Haensel P., Meyer J., Schaeffer R., 1998b, Nucl. Phys. A, 635, 231
Chamel N., Carter B., 2006, MNRAS, 368, 796
Chamel N., Haensel P., 2006, Phys. Rev. C, 73, 045802
Comer G. L., Joynt R., 2003, Phys. Rev. D, 68, 023002
Dean D. J., Hjorth-Jensen M., 2003, Rev. Mod. Phys., 75, 607
Easson I., 1979, ApJ, 233, 711
Easson I., Pethick C. J., 1979, ApJ, 227, 995
Farine M., Pearson J. M., Tondeur F., 2001, Nucl. Phys. A, 696, 396
Ginzburg V., Kirzhnits D., 1965, Sov. Phys. JETP, 20, 1346
Glendenning N. K., 2000, Compact Stars: Nuclear Physics, Particle Physics, and General Relativity. Springer, New York
Gourgoulhon E., 2006, in Rieutord M., Dubrulle B., eds, EAS Pub. Ser. Vol. 21, Stellar Fluid Dynamics and Numerical Simulations: From the Sun to Neutron Stars. EDP Sciences, Cambridge, p. 43
Haensel P., Potekhin A. Y., 2004, A&A, 428, 191
Haensel P., Potekhin A. Y., Yakovlev D. G., 2006, Neutron Stars 1: Equation of State and Structure. Springer, New York
Heiselberg H., Hjorth-Jensen M., 2000, Phys. Rep., 328, 237
Israel G. L. et al., 2005, ApJ, 628, L53
Lassaut M., Flocard H., Bonche P., Heenen P. H., Suraud E., 1987, A&A, 183, L3
Lattimer J. M., Prakash M., 2007, Phys. Rep., 442, 109
Lattimer J. M., Pethick C. J., Ravenhall D. G., Lamb D. Q., 1985, Nucl. Phys. A, 432, 646
Lattimer J. M., Prakash M., Pethick C. J., Haensel P., 1991, Phys. Rev. Lett., 66, 2701
Lesinski T., Bennaceur K., Duguet T., Meyer J., 2006, Phys. Rev. C, 74, 044315
Lin L.-M., Andersson N., Comer G. L., 2007, preprint (arXiv:0709.0660)
Lorenz C. P., Ravenhall D. G., Pethick C. J., 1993, Phys. Rev. Lett., 70, 379
Lunney D., Pearson J. M., Thibault C., 2003, Rev. Mod. Phys., 75, 1021
Margueron J., Navarro J., van Giai N., 2002, Phys. Rev. C, 66, 014303
Misner C. W., Thorne K. S., Wheeler J. A., 1973, Gravitation. W. H. Freeman and Co., San Francisco
Muther H., Prakash M., Ainsworth T. L., 1987, Phys. Lett. B, 199, 469
Negele J. W., Vautherin D., 1972, Phys. Rev. C, 5, 1472
Rayet M., Arnould M., Paulus G., Tondeur F., 1982, A&A, 116, 183
Samuelsson L., Andersson N., 2007, MNRAS, 374, 256

Steiner A. W., Prakash M., Lattimer J. M., Ellis P. J., 2005, Phys. Rep., 411, 325
Stone J. R., Reinhard P.-G., 2007, Prog. Part. Nucl. Phys., 58, 587
Strohmayer T. E., Watts A. L., 2005, ApJ, 632, L111
Strohmayer T. E., Watts A. L., 2006, ApJ, 653, 593
van Dalen E. N. E., Fuchs C., 2007, Eur. Phys. J. A Suppl., 31, 29
Vautherin D., Brink D. M., 1972, Phys. Rev. C, 5, 626
Villain L., Haensel P., 2005, A&A, 444, 539
Watts A. L., Strohmayer T. E., 2006, ApJ, 637, L117
Watts A., Krishnan B., Bildsten L., Schutz B., 2008, MNRAS, submitted (arXiv:0803.4097)
Woods P. M., Thompson C., 2006, in Walter L. and van der Klis M., eds. Cambridge Astrophys. Ser. 39, Compact Stellar X-ray Sources. Cambridge Univ. Press, Cambridge, p. 547
Yakovlev D. G., Pethick C. J., 2004, ARA&A, 42, 169
Yakovlev D. G., Kaminker A. D., Gnedin O. Y., Haensel P., 2001, Phys. Rep., 354, 1
Zuo W., Lombardo U., Schulze H.-J., Li Z. H., 2006, Phys. Rev. C, 74, 014317

This paper has been typeset from a TEX/LATEX file prepared by the author.